

AD-A093 702

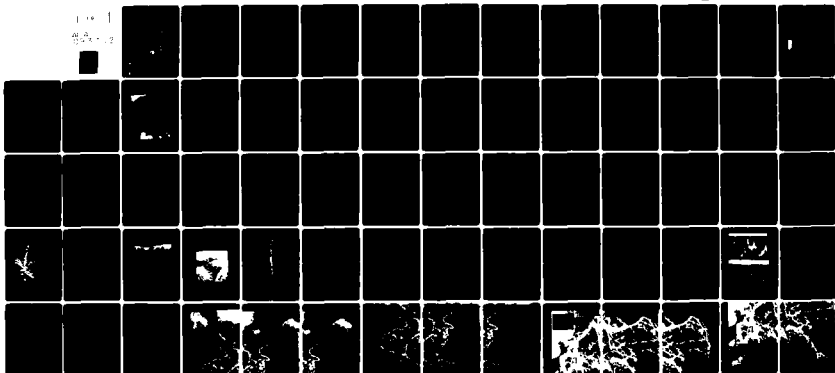
NAVAL OCEAN RESEARCH AND DEVELOPMENT ACTIVITY NSTL S--ETC F/6 8/10  
AN APPROACH TO THE QUANTITATIVE STUDY OF SEA FLOOR TOPOGRAPHY.(U)  
JAN 80 J E MATTHEWS

UNCLASSIFIED

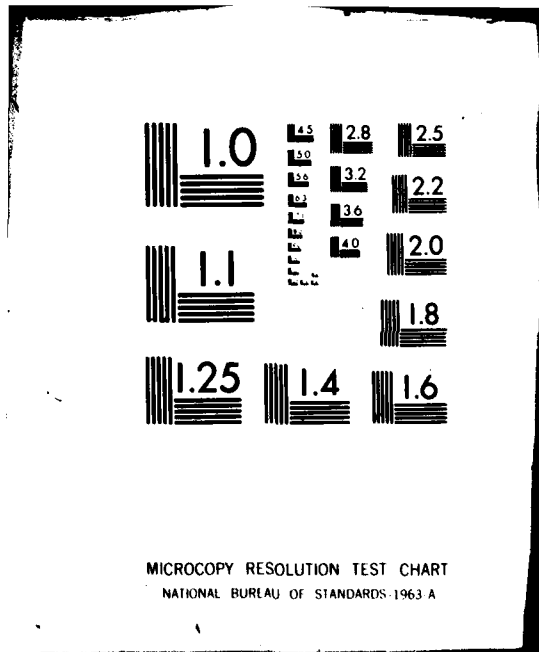
NORDA-TN-47

NL

1-1  
80-1-2



END  
DATE  
FILMED  
2 83  
DTIC



MICROCOPY RESOLUTION TEST CHART  
NATIONAL BUREAU OF STANDARDS-1963 A

NORDA Technical Note 47

BS (1)

AD A093702

# An Approach to the Quantitative Study of Sea Floor Topography

J. E. Matthews

# LEVEL II

Sea Floor Division  
Ocean Science and Technology Laboratory

January 1980

*See 1473 on back*

DTIC  
ELECTE  
JAN 13 1981  
S D  
E



DISTRIBUTION STATEMENT A  
Approved for public release  
Distribution Unlimited

NAVAL OCEAN RESEARCH AND DEVELOPMENT ACTIVITY  
NSTL Station, Mississippi 39829

FILE COPY

81 1 12 021

## EXECUTIVE SUMMARY

This report represents an assessment of sea floor and sub-sea floor relief as related to acoustic bottom interaction. Marine topography, whose amplitude spans six orders of magnitude, is here divided into three broad categories: (1) features likely to cause propagation blockage, (2) features which act as sloping bottoms, and (3) features which act as acoustic scatterers. Maps of the North Atlantic and North Pacific Oceans are presented which delimit the areas where each of these three categories would be expected to dominate propagation.

It is recommended that features causing blockage be dealt with in a deterministic manner based upon the best available bathymetry. Features producing a sloping bottom are often too small to be dealt with as individuals, and therefore have been dealt with statistically. It is demonstrated that this scale of relief can, at least as a first approximation, be treated as a stationary, stochastic process consisting of colored noise with a Gaussian distribution. A statistical model of features which act as scatterers was not developed. This class of relief, because of its size, requires stabilized, narrow-beam or deep-towed bathymetry for accurate definition. These features are the result of igneous, sedimentary and tectonic processes, and must, when collectively dealt with, have nonstationary statistics. For these two reasons, it is recommended that a more detailed assessment of acoustic requirements be made before major studies of this scale of relief are undertaken.

Accession For	
NTIS GRA&I	<input checked="" type="checkbox"/>
DTIC TAB	<input type="checkbox"/>
Unannounced	<input type="checkbox"/>
Justification	
By _____	
Distribution/	
Availability Codes	
Dist _____	
<b>A</b>	

#### ACKNOWLEDGEMENTS

This study was carried out with the support of Naval Electronic Systems Command Code 320, under their Acoustic Bottom Interaction Program. S. Madosik and L.G. Hemler assisted in data reduction. Discussion with D.W. Handschumacher, K.E. Gilbert and J. Egloff have been most helpful during the analysis and interpretative phases of the investigation. T.L. Holcombe and Peter Fleischer critically reviewed, and L. McRaney edited, the final manuscript.

## CONTENTS

	PAGE
I. INTRODUCTION	1
II. SCALE LIMITS OF TOPOGRAPHY APPLICABLE TO LOW FREQUENCY ACOUSTICS	2
III. DETERMINISTIC APPROACH TO TOPOGRAPHY	6
A. North Atlantic Relief	6
B. North Pacific Relief	8
C. Synthesis	11
IV. STATISTICAL APPROACH TO TOPOGRAPHY	13
A. Basaltic Relief	15
B. Sediment Modification to Basaltic Relief	20
V. CONCLUSIONS	22
VI. REFERENCES	27
APPENDICES	
APPENDIX A: ORIGINS OF SEA FLOOR TOPOGRAPHY	29
APPENDIX B: DEPTH-DISTANCE ACCURACY DEPENDANCE UPON TIME TO DISTANCE AND A/D CONVERSION	42
APPENDIX C: ERRORS RESULTING FROM ECHO SOUNDER BEAMWIDTH	45
PLATE I. North Atlantic Relief Map	Back Pocket
PLATE II. North Pacific Relief Map	Back Pocket

## ILLUSTRATIONS

	PAGE
FIGURE 1. Minimum amplitude for surface roughness affecting acoustic scattering based upon the Rayleigh criterion for frequencies of 10 and 100 Hz.	4
FIGURE 2. Width of three Fresnel zones for frequencies of 10 and 100 Hz.	5
FIGURE 3. North Atlantic feature names. Shaded areas correspond to areas of high relief in Plate I.	7
FIGURE 4. North Pacific feature names. Shaded areas correspond to areas of high relief in Plate II.	10
FIGURE 5. Ratio of surface-to-basement RMS relief versus sediment thickness.	21
FIGURE 6. (A) Depth of the basaltic basement versus distance from the spreading axis for various spreading rates.	32
(B) Theoretical relief difference across a fracture zone versus age of younger plate for various age differences.	32
FIGURE 7. Generalized amplitude and width ranges of common sea floor features. Straight line trends indicate amplitude as an exponential function of wave number with the indicated power.	35
FIGURE 8. Diagrammatic representation of the sea floor showing the major tectonic and sedimentary features encountered in deep ocean basins.	36
FIGURE 9. Vertical reflection seismic record of sand waves which comprise the Lower Continental Rise Hills off the east coast of North America.	38
FIGURE 10. Deep-sea photograph showing the top of the basaltic layer ponded sediments. The ripple marks and their diffraction patterns around the basalt "pillows" give verification of bottom current activity.	39
FIGURE 11. Vertical reflection seismic record showing the typically rough basaltic basement covered by hemipelagic sediments. The configuration of the water-sediment interface results from the combined effects of rough basement and bottom current activity.	40
FIGURE 12. A hypothetical, two-dimensional sea floor composed of geometrical shapes, and its associated computed echogram. Constructed from Krause (1962).	47
FIGURE 13. Comparison of wide ( $30^\circ$ ) versus narrow ( $2^\circ$ ) beam width echo sounder over the same bottom.	48

## I. INTRODUCTION

The operation of many sonars is to some extent dependent upon the interaction of acoustic signals with the sea floor. Seafloor morphology is, however, one area of marine environmental research which has not undergone broad, quantitative investigation in relation to marine acoustics, although a number of specific studies have been published. It is the purpose of this report to discuss morphology with acoustical implications in mind, specifically, in relation to long-range acoustic propagation.

Sea-floor features span six orders of magnitude in size, from ripple marks with relief of centimeters to continental margins with relief of kilometers. The discussion to follow will attempt to put this entire size range of features into a generalized acoustical context, and, where possible, to derive quantitative descriptions to serve as guidelines for future acoustic investigations.

Early seismic refraction profiles revealed stratification within the oceanic crust. "Seismic layer one" was thought to be sediment and "seismic layer two" was thought to be basalt. Drilling has since confirmed this interpretation, and vertical seismic reflection profiles have provided a broad view of the configuration of the water-sediment and sediment-basalt interfaces. Two broad categories of sediment provinces are of significance to acoustic bottom interaction. In thin pelagic sediments (lutites or oozes), the acoustic impedance mismatch at the water-sediment interface is generally not great, and attenuations are low, so much of the incident energy is transmitted down to interact with the high impedance basaltic surface. On the other hand, in thick sediment sections such as turbidites, positive velocity gradients in the sediment layer refract the acoustic energy back before it can reach the deeply buried basaltic basement.

Sea floor and sub-sea floor interfaces generally affect acoustic bottom interaction in one of three ways: (1) small features collectively produce a rough surface which causes scattering and loss of signal coherence; (2) intermediate size features are only partially insonified and act as bottom slopes, causing bearing and range errors as well as complex reflection phenomena; and (3) the largest features block acoustic propagation. A study of sea-floor morphology in terms of acoustic bottom interaction must, therefore, first define the dominant type of interaction in a given region; i.e., scattering is of little importance if a seamount completely blocks transmission, or roughness of the basaltic surface is of little importance if the interface is too deeply buried to interact.

Only order of magnitude size limits are established in this paper to separate the above categories of relief. Features large enough to cause acoustic blockage have, for the most part, been mapped, and their position and configuration can be determined from the best available bathymetric maps. Intermediate size features, which produce bottom slope, are detected on echo sounder and seismic records, but many are too small to be mapped as individuals. The smallest group of features, those causing acoustic scattering, are generally detected only by stabilized, narrow-beam or deep-towed echo sounders, and these data are in short supply. Of these three sizes of features, the first group lends itself to a deterministic treatment (mapping); the latter two groups are deterministic, but because of their size, a statistical approach is suggested in lieu of the tremendous effort that would be required to map them as individuals over large areas. Even if mapping of these smaller features were possible, it may not be the desired solution, since many theoretical acoustic treatments or engineering applications require an input of statistical parameters to describe the interface.

The majority of previous marine morphological studies have been of a qualitative nature, but a few investigators have made statistical measures of bottom depth or bottom slope. These studies are cited and their conclusions reviewed. This review of the existing literature, however, does not provide a definitive view of sea floor topography for use by the acoustic community.

Two general approaches were used in the current study to classify relief. One approach consisted of a regional classification of North Atlantic and North Pacific relief derived from the best available bathymetry maps, while the other consisted of statistical analysis of echo sounder and seismic reflection records from the two oceans. In the first approach, a digital data base was constructed which contains the maximum, minimum, and mean depth in 30 x 30 nautical mile (56 km) squares. These data were analyzed and three categories of relief were finally chosen to depict the regional morphology of the two oceans (Plates I and II). The highest relief category (greater than 1900 m) essentially depicts areas where propagation blockage is likely to occur. The two categories of lower relief (1100-1900 m and 0-1100 m) depict areas where acoustic scattering and slope problems will occur. These two categories of lower relief were chosen to demonstrate the significant differences between the two oceans. The intermediate scale is prominent in the North Atlantic, and possibly results from the closely spaced fracture zones of that ocean. This intermediate scale of relief is far less prominent in the North Pacific where fracture zone spacing is an order of magnitude greater.

To quantitatively assess the characteristics of the two lower relief categories, selected echo sounder and seismic reflection records from both oceans were digitized and their statistics computed. This analysis was applied to both the water-sediment and sediment-basalt interfaces for wavelengths greater than a few kilometers. Preliminary indications are that these interfaces can be treated as though they were random noise with a Gaussian depth distribution, and a depth power spectrum that can be represented by wave number to the -1.8 power. Furthermore, the North Atlantic Ocean is significantly rougher than the North Pacific Ocean with average RMS roughnesses of 259 m and 99 m, respectively. This difference in roughness could not, in the present study, be attributed to differences in sea floor spreading rates. This does not, however, preclude a spreading rate threshold, below which a significant change in relief-forming mechanisms may occur.

Features with wavelengths of less than a few kilometers overlap the size range of acoustic scatters and require very narrow beam, stabilized echo sounders or bottom-towed devices for their accurate definition. This class of features will be far more difficult to deal with on a global scale because of the limited areal coverage by these high resolution devices. For that reason, these features were not investigated in the current study.

## II. SCALE LIMITS OF TOPOGRAPHY APPLICABLE TO LONG RANGE ACOUSTICS

A great deal of material has been published on the subject of wave scattering by rough surfaces. Whether it be scattering of electromagnetic or acoustic waves, the theory is essentially the same, and was first discussed quantitatively by Lord Rayleigh (1945). He formulated a relationship, now known as the "Rayleigh criterion," which somewhat arbitrarily defines what amplitude surface irregularities must be to define the surface as rough. This criterion is an inequality relating roughness amplitude (h) to grazing angle ( $\theta$ ) and acoustic wavelength ( $\lambda_A$ ),

$$h > \frac{\lambda_A}{8 \sin \theta} \quad (1)$$

There are other criteria for distinguishing smooth from rough surfaces that have been presented as being more "realistic," but it is not the purpose of the present discussion to press for a more exact definition. The purpose here is to define only generalized limits of the area of interest. Figure 1 presents the minimum height of roughness ( $h$ ) defined by the above inequality versus grazing angle for wavelengths between 15 and 150 m (10 to 100 Hz frequencies for a sound speed of 1500 m/s). It should be noted, however, that the Rayleigh criterion is independent of roughness wavelength.

At the other size extreme, if the area of acoustic insonification covers only one side of a feature, the feature would not act as a scatterer, but as a sloping surface. Therefore, if  $\lambda_R$  represents the roughness wavelength, and  $D_I$  represents the dimension of the insonified area, then

$$D_I \approx \lambda_R/2 \quad (2)$$

This relationship could be used to define the boundary between features that act as acoustic scatterers, and features that represent sloping bottoms. The problem now becomes one of determining the size of the insonified area. Beckmann and Spizzichino (1963) discuss this problem, and state: "The widely accepted answer to this question is 'the first few Fresnel zones'. We have no better answer to offer; however, for oblique incidence the above statement is not evident at all and has, to the present writer's knowledge, never been rigorously demonstrated." Here again, rigorously devised criteria do not exist, but general limits of the area of interest can be estimated.

For a point source and receiver occupying the same location, the Fresnel zones are concentric circles. For separated source and receivers the Fresnel zones become ellipses, which are concentric only if source and receiver are at the same distance from the reflecting surface. An additional complicating factor is that for the oblique reflection case, where source and receiver are at different heights above the reflecting surface, the amplitude of excitation is not symmetric about the direction of propagation. Thus, for the sake of simplicity, acceptance of the first few Fresnel zones (the first three Fresnel zones were chosen for the present discussion) as the insonified area is here adopted. Beckmann and Spizzichino (1963) derive analytical expressions for the semi-major and semi-minor axes of the Fresnel zones at oblique reflection, but these are dependent upon the source-receiver geometry. Therefore, a plane wave approximation of the first three Fresnel zones is here used for an approximation of the dimensions of the insonified area in the deep ocean. For the plane wave case, the zones become parallel bands extending to infinity perpendicular to the direction of propagation. This is similar to the familiar interference patterns produced by propagating light through two parallel slits. The approximation, although crude, illustrates the importance of grazing angle upon the dimensions of the first three Fresnel zones, which is illustrated in Figure 2 for wavelengths of 15 and 150 m (10 and 100 Hz at a sound speed of 1500 m/s).

The limiting criterion illustrated in Figures 1 and 2 can be used to bound the range of feature sizes of interest to low-frequency acoustic scattering and bottom slope. (Low frequency is here defined as the order of magnitude of frequencies between 10 and 100 Hz.) The angle of critical reflection is commonly less than  $10^\circ$  for the deep ocean environment. However, bottom interaction measurements indicate that at low frequencies, the energy loss from bottom interactive acoustic paths can, in some cases, be at or near zero loss for grazing angles of  $30^\circ$  or more.

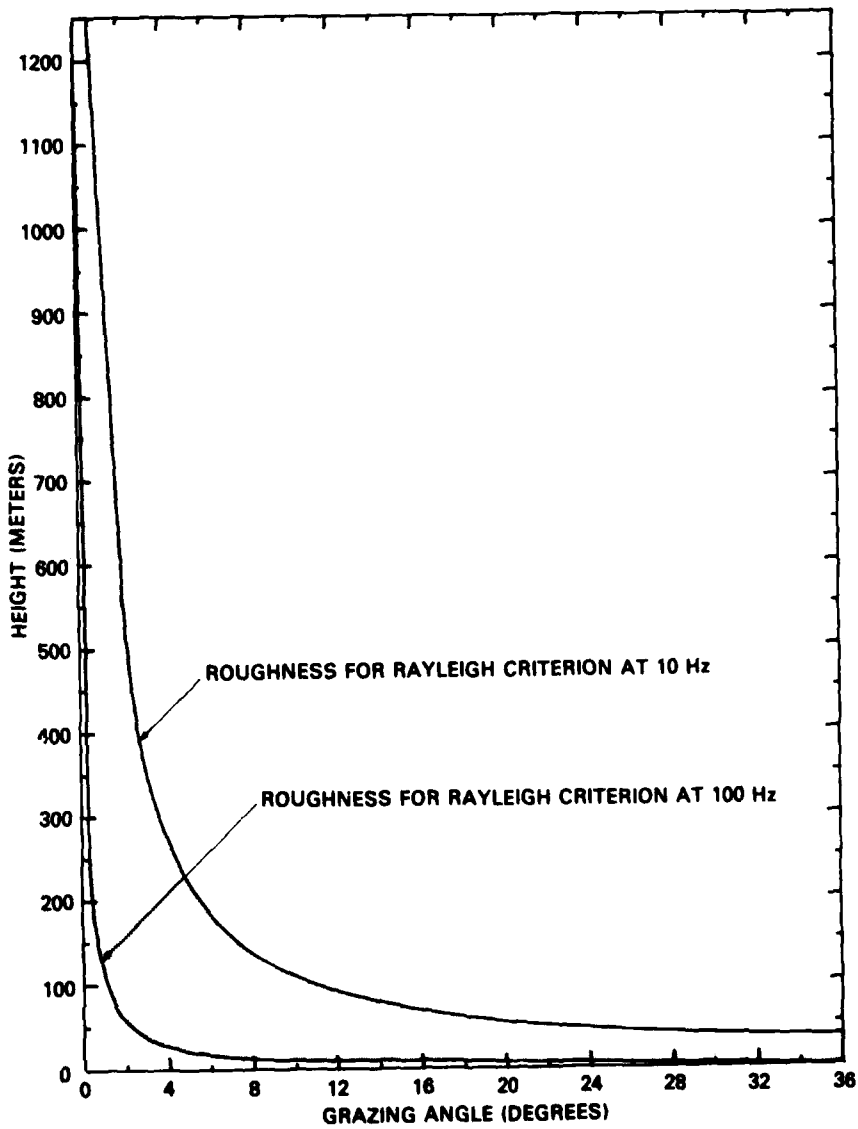


Figure 1. Minimum amplitude for surface roughness which affects acoustic scattering based upon the Rayleigh criterion for acoustic frequencies of 10 and 100 Hz. Wave velocity assumed to be 1500 m/s.

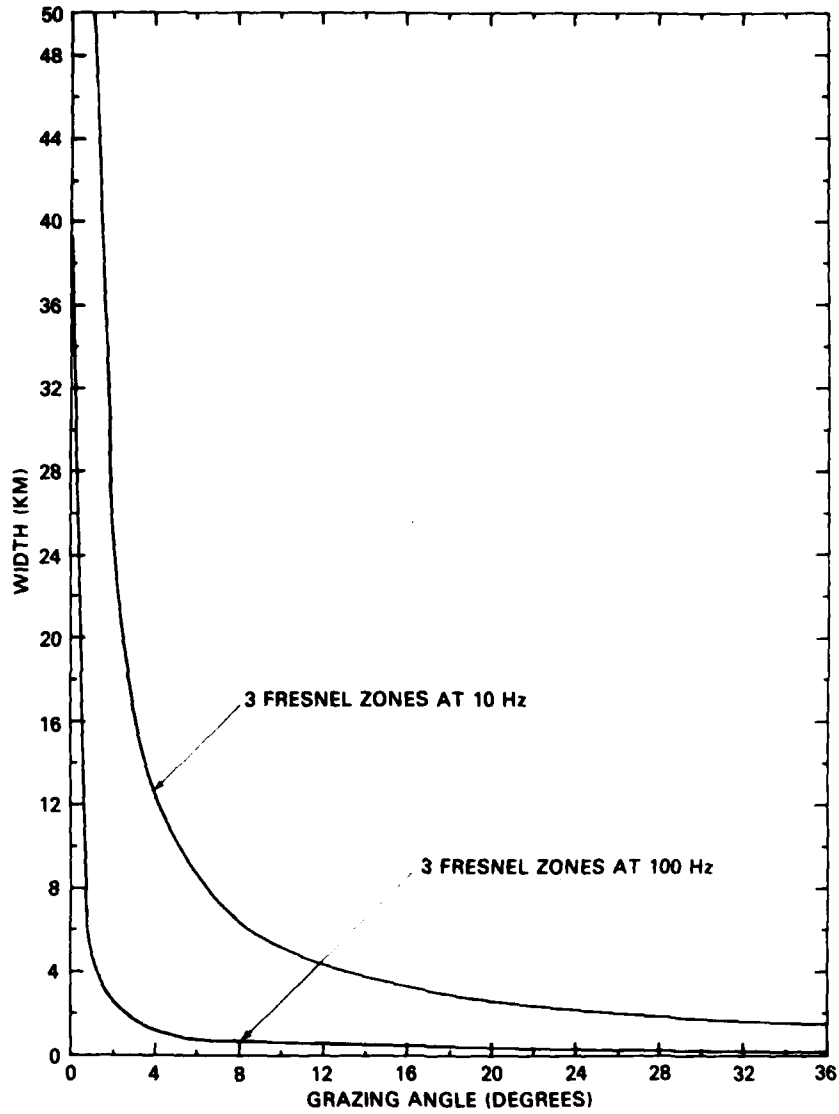


Figure 2. The width of three Fresnel zones (in kilometers) for frequencies of 10 and 100 Hz. Based upon an acoustic wave velocity of 1500 m/s using a plane wave incident upon the interface.

Therefore, an acoustic wavelength range of 15-150 m at grazing angles of 0-30° is considered to be the range of interest for the present study. Thus, sea-floor features with amplitudes greater than 1-100 m, and wavelengths of less than several kilometers, are in the range applicable to scattering, while the longer wavelengths have application to sloping bottom problems. The feature size applicable to acoustic blockage is not dependent upon acoustic wavelength or grazing angle. Blockage is dependent upon ocean depth, feature height above the surrounding depth, and water column sound speed structure. To make a general statement based upon observation, blockage in the deep ocean commonly occurs when a feature rises two to three kilometers above the sea floor. Further definition would require specification of geographic location and source-receiver geometry. The classification of marine morphology is primarily generic rather than by just size; however, the general size range for scatterers is roughly coincident with that of the abyssal hills or smaller, features affecting slope are the size of abyssal hills or larger, and blockage results from seamounts.

### III. DETERMINISTIC APPROACH TO TOPOGRAPHY

Previous studies indicate that the statistics of sea floor topography vary, thus, marine morphology should be treated as a nonstationary stochastic process. This is consistent with geological observations that the configuration of the sea floor is the result of a combination of mutually independent mechanisms, each with an independent spatial variation.

To investigate the largest sea floor features, the North Atlantic and North Pacific Ocean Basins were divided into 30 x 30 nautical mile (nm) squares (56 km), and the maximum, minimum, and mean depth for each square was determined.\* On the basis of subsequent analysis, relief ranges of 0-1100, 1100-1900 and greater than 1900 m were chosen, and relief maps of the North Atlantic and North Pacific Oceans were produced. The results of this compilation are presented in plates I and II.

The most striking characteristic of the two plates is the difference between the two oceans. The North Atlantic has only a small percentage of area containing high relief (greater than 1900 m relief); the remainder is almost equally divided between intermediate (1100-1900 m relief) and low relief (less than 1100 m relief). On the other hand, the North Pacific is predominantly high or low relief, with only a small percentage of intermediate relief which appears only as a transition zone between areas of high and low relief.

#### A. NORTH ATLANTIC RELIEF

Aside from the continental margins, crest of the Mid-Atlantic Ridge, Azores-Gibraltar Ridge, Southeast Newfoundland Ridge and Kings Trough, North Atlantic high relief is associated with only a few island groups (Fig. 3). There is only one seamount chain in the North Atlantic Ocean. Of the fracture zones, only the CHARLIE, OCEANOGRAPHER, KANE, and VEMA have relief in excess of 1900 m, and even then, it is restricted to that portion very near the ridge crest. Aside from the area between the ridge crest and the Iberian Peninsula (in the vicinity of the Azores-Gibraltar Ridge and Kings Trough), the intermediate relief is restricted to the flanks of the ridge. The width of the zone of intermediate relief varies from

\*NOTE: This data base is being made available in digital form through the National Geophysical and Solar-Terrestrial Data Center (NGSDC) of the National Oceanic and Atmospheric Administration, Boulder, Colorado.

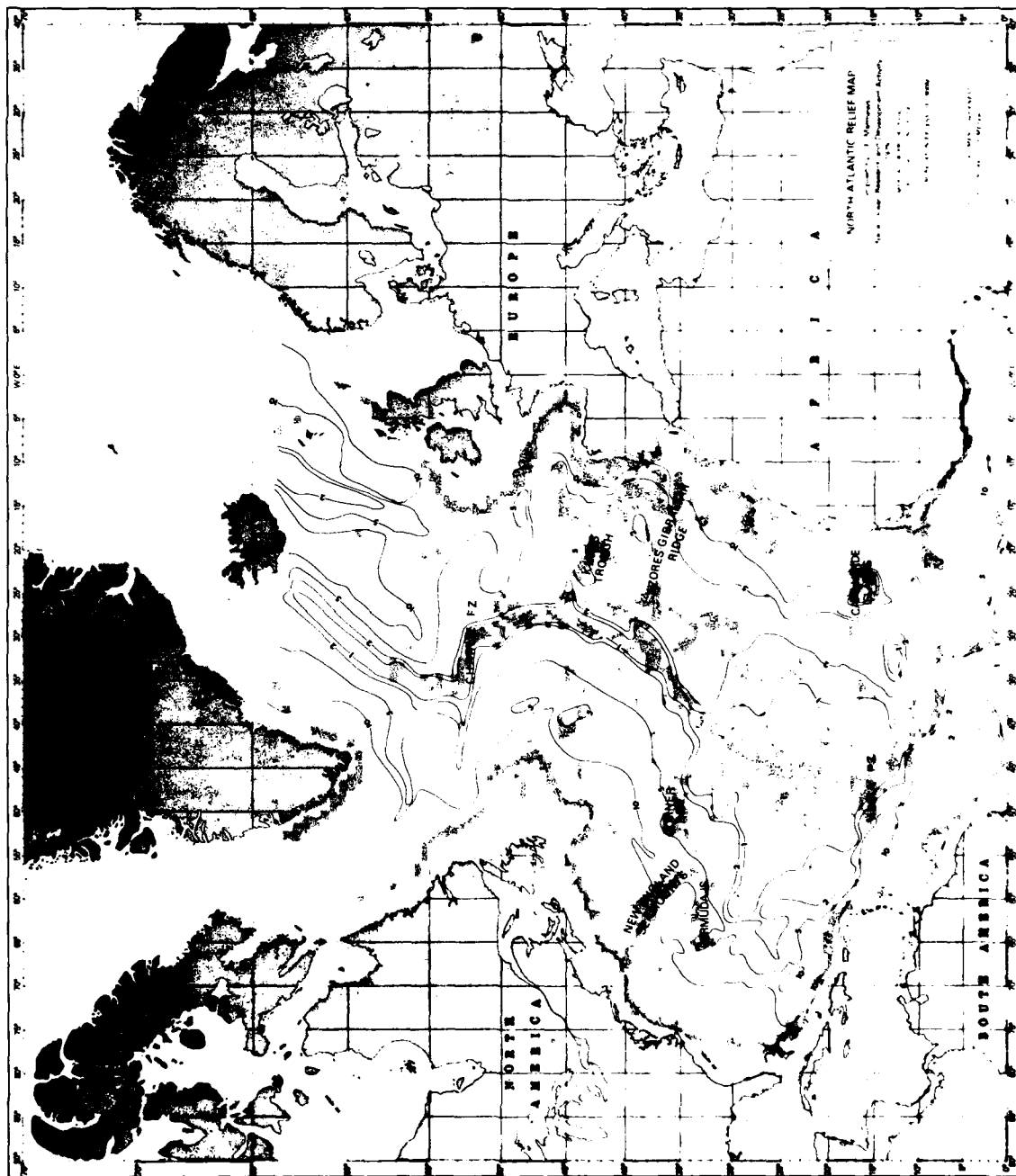


Figure 3. North Atlantic Ocean feature names. Shaded areas depict the high relief category of Plate I.

16 to 390 km on either side of the ridge crest. Generalized contours of total sediment thickness shown on Plate I (Ewing et al., 1973) explain the variable width of this zone. The ridge crest and flanks south of 35°N have a thin veneer of sediment which leaves the rough basaltic basement virtually exposed.

The area of thin sediment (a corresponding zone exists in the South Atlantic) coincides with present-day zones of low biological productivity as defined by Be' and Tolderlund (1971). This explanation would require long-term stability of the present productivity pattern. Global productivity of pelagic organisms is heavily dependent upon nutrient-rich polar waters, the circulation patterns of which could well be invariant for a span of geologic time. Another mechanism producing a depositional boundary geographically coincident with biological productivity is the southern limit of Pleistocene ice rafting. As icebergs from the continental ice sheets drifted south, they melted, depositing their loads of silt, sand, and gravel to produce what are known as glacial-marine sediments. Ruddiman (1977) and references cited in that paper document a significant contribution of glacial material to North Atlantic sediments north of approximately 40°N. Still another factor contributing to sediment distributions of the North Atlantic is the influence of bottom currents. Jones et al. (1970) demonstrated the influence of sporadic overflows of dense Norwegian Sea water upon deep currents and near-bottom sediment transport. This southward flow of bottom water along the east side of the Mid-Atlantic Ridge deposits thick sediment drifts on the ridge flank. Leakage through fracture zones also supplies large amounts of sediment to the western flank of the ridge. Upon encountering the Charlie Fracture Zone at about 52°N, the bulk of the flow and sediment transport is diverted to the western side of the ridge. After making a large loop into the Labrador Basin, the flow follows the western flank of the ridge onto the south where it becomes known as North Atlantic Deep Water. The flow causes smaller, but significant, sediment drifts on the western flank of the ridge south of the Charlie Fracture Zone. Again the flow is diverted at about the Oceanographer Fracture Zone. From this point south, the North Atlantic Deep Water follows the continental margin of North America, well clear of the Mid-Atlantic Ridge.

The area of thin sediment is slightly asymmetric with respect to the ridge crest, with the zone extending farther on the western ridge flank. This results from elevated basaltic basement associated with the Bermuda Rise and Corner Rise. This basement elevation has protected the region from the influence of such topographically controlled sediment deposits as turbidites and the previously discussed sediment drifts associated with Atlantic Deep Water. The eastern and western margins of the North Atlantic Ocean Basin are characterized by a kilometer or more of continentally derived sediments which form coalescing abyssal plains.

The North Atlantic Ocean floor is thus characterized by: (1) small areas of high relief associated with the ridge crest, large fracture zones and scattered island groups, (2) a significant amount of intermediate scale relief associated with areas of thin sediment cover on the ridge flanks, and (3) significant areas of low relief associated with sediment thicknesses sufficient to mask the underlying basaltic roughness.

## B. NORTH PACIFIC RELIEF

The North Pacific Ocean (Plate II) is almost equally divided between areas of high and low relief. The less dominant, intermediate relief forms only a fringe around the high relief areas, or connects areas of high relief to form linear relief trends. There are no broad expanses of intermediate relief as found in the North

Atlantic Ocean. North Pacific high relief is primarily associated with fracture zones, seamounts, and island arc-trench systems.

The direct contribution to topography by a spreading ridge in the North Pacific Ocean is relatively minor. Almost the entire ocean floor is formed by a single plate, the Pacific Plate. Only two portions of the spreading ridge lay north of the equator, the northern tip of the East Pacific Rise (inset on Plate II) and the Juan de Fuca/Gorda Ridge shown in Figure 4. The remainder of the eastern North Pacific high relief is associated with the Mendocino, Murray, Molokai, Clarion, and Clipperton Fracture Zones. The northeastern North Pacific has high relief associated with the Chinook and Sila Fracture Zones, Emperor Trough, and Kodiak Seamount Chain. In this region there are also north-south high relief trends just to the south of the Aleutian Trench which are related to unnamed fracture zones in that region.

These eastern and northern portions are separated from the remainder of the North Pacific Basin by the Emperor Seamount Chain, Hawaiian Ridge, and Line Island Ridge, all of which are high relief trends. The northwestern North Pacific, between the Emperor Seamount Chain and the Japan-Kuril-Kamchatka Trench, is called the Northwest Pacific Basin, and has high relief only in association with the Shatsky Rise. West of approximately 145°E, the North Pacific Ocean has predominantly high relief, with only the Caroline, Philippine, Mariana Back Arc, and Shikoku Basins having low relief. The remainder of the North Pacific (bounded by the Palau-Mariana Arc, Line Island Ridge and Northwest Pacific Basin) consists of a rather complex network of seamount-island chains of high relief, and inter-island basins of low relief.

The sediments of the North Pacific are generally less than 400 m in thickness. This is shown by the contours in Plate II, which were modified from Morton and Lowrie (1978), Heezen and Fornari (1975), and Ewing et al. (1968). Most of the large land masses capable of providing significant contributions of detrital sediment to the basin are separated from the basin by trenches. Only the western margins of the United States and Canada have abyssal plains where sedimentation rates are high and the bordering trench appears to have been buried (Riddiough, 1978). A portion of this margin is blocked from the Pacific Basin by the Juan de Fuca Ridge. With the exception of these abyssal plains and deep sea fans off the west coast of North America, the North Pacific Basin is covered with pelagic sediment. There is a small amount of glacial-marine sediment north of about 45°N (Kent et al., 1971). Volcanic ash layers contribute little to the volume of Pacific sediments; however, montmorillonite clays derived from volcanogenic material and silt- to sand-sized grains derived from basalt and andesite do, in places, constitute a significant portion of the otherwise pelagic sediment.

The majority of the North Pacific is covered by illite clays (derived from wind-transported, chemically weathered continental rocks), and the tests of siliceous and calcareous pelagic animals. An equatorial zone of sediment thickening is caused by high productivity of carbonate organisms, coupled with a decreased carbonate compensation depth in the low latitudes. A slight thickening in the northern portion of the Pacific Basin results from increased productivity of siliceous animals, coupled with their generally low solubility. The remainder of the basin is covered by "red clay" which slowly thickens with crustal age in a westerly direction. There is anomalously thick sediment associated with elevated regions such as the Mid-Pacific Mountains, Shatsky Rise, and Emperor Seamounts, resulting from their elevation above the carbonate compensation depth.

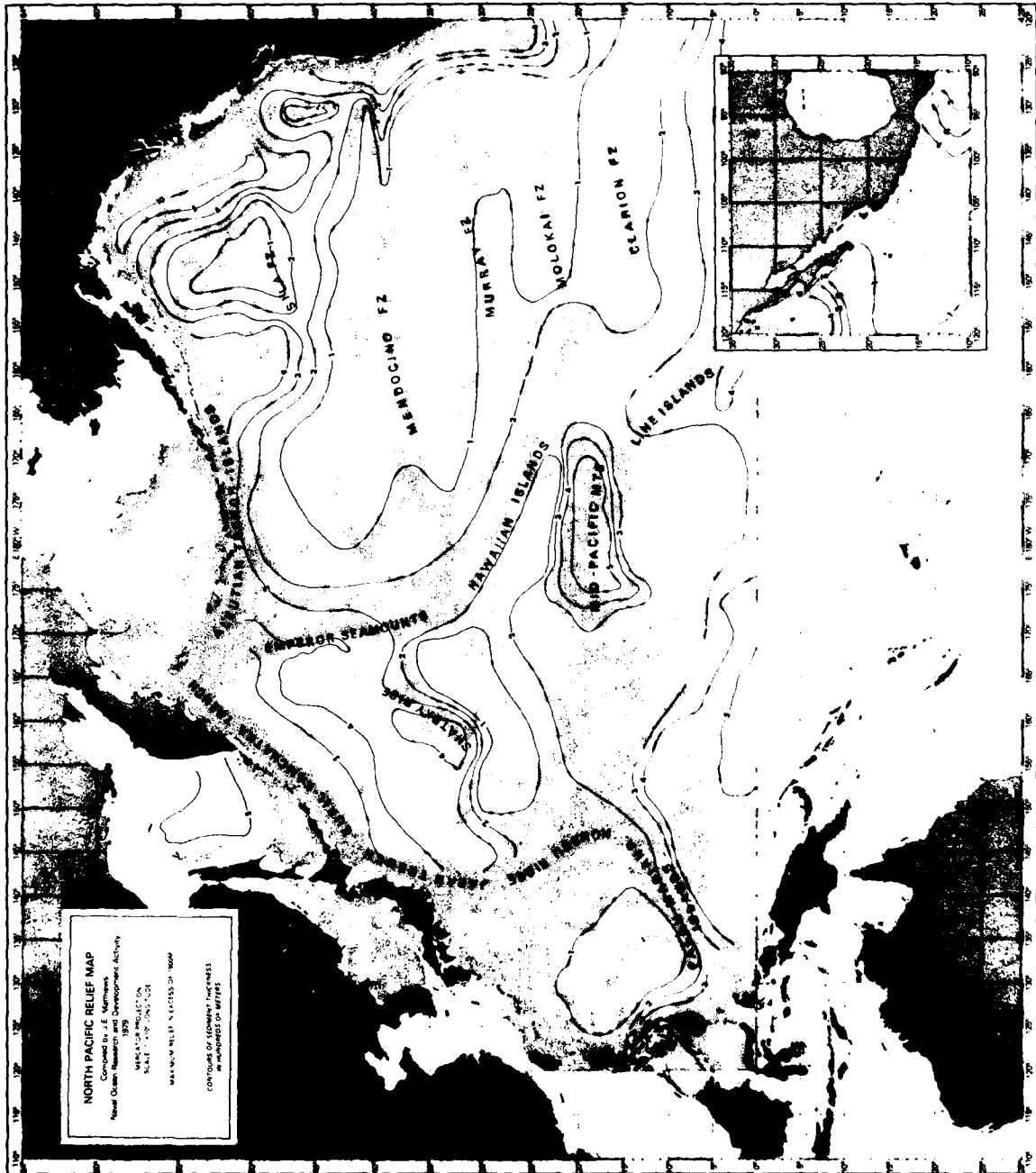


Figure 4. North Pacific Ocean feature names. Shaded areas depict the high relief category of Plate II.

The generally thin sediment cover typical of the North Pacific is found only on the ridge crest north of 35°N, and on the ridge crest and ridge flanks to the south, in the North Atlantic Ocean. These areas of thin sediment in the Atlantic, however, are associated with intermediate roughness. In the remainder of the North Atlantic, thicker sediment appears to account for the reduced surface relief. In the North Pacific, on the other hand, the thin sediment is associated with low relief. It thus appears that the North Pacific Ocean has a significant amount of high relief associated with seamounts and fracture zones, but lacks the intermediate relief associated with the North Atlantic in areas of comparable sediment thickness.

### C. SYNTHESIS

The distributions of relief depicted in Plates I and II indicate a significant difference between the North Atlantic and North Pacific Ocean Basins. Plate tectonic theory has not yet evolved to the point where these differences can be attributed to specific mechanisms, but spreading rate differences and plate boundary influences have been proposed as general explanations.

The North Atlantic Basin is composed of two plates symmetrically positioned relative to a central, slowly spreading ridge. The continents of Europe, Africa, and the Americas are "welded" to and move with these two North Atlantic plates. This has left the Atlantic Basin margins tectonically quiet and relatively stable throughout their history (with the exception of a short zone of subduction in the Caribbean region). The North Pacific, on the other hand, consists almost entirely of a single plate and much of the spreading ridge is approaching, or has already been subducted, beneath the Americas. The western and northern boundaries of this plate are formed by a continuous band of coalescing trenches where the plate is being subducted. Throughout much of its history, the North Pacific Basin has been formed by fast spreading, probably with significant tectonic activity at its margins, while the North Atlantic Basin has been formed by slow spreading with very little tectonic activity along its margins.

The North Atlantic basaltic basement consists predominantly of relief in the intermediate range, and has closely spaced fracture zones. With the exception of a few small, localized areas of high relief (Bermuda, New England Seamount Chain, etc.), the only other anomalous features are between the ridge crest and the Iberian Peninsula. This area is dominated by intermediate and high relief, probably caused by a secondary axis of spreading (Ridley et al., 1974). This disruption explains the Azores-Gibraltar Ridge and differences in the spreading direction above and below this latitude. The slow symmetric spreading of the Mid-Atlantic Ridge has tended to produce crust with intermediate relief and closely spaced fracture zones. The absence of tectonic interaction with continents on the basin margins has probably tended to minimize the formation of anomalous features of high relief. An unknown force, probably external to the Atlantic crust, such as a shift in the pole of rotation or shift in mantle convection, has caused a single major zone of high relief in the area of the Azores-Gibraltar Ridge. The areas of North Atlantic low relief result from sediment accumulation of sufficient thickness to mask the intermediate relief of the basaltic surface beneath.

The North Pacific can be divided into three areas of dissimilar topography. The line formed by the Emperor-Hawaiian-Line Island chain of seamounts has been termed the ICSU Ridge (named for the International Council of Scientific Unions, the sponsors of International Geophysical Year). To the east of this line, the crust is relatively smooth, apparently a result of having been formed by a fast spreading ridge. This portion of the Pacific contains long, widely spaced fracture

zones with associated high relief produced by secondary block faulting associated with the zones. These large fracture zones range from 900 to 5500 km in length, and from 500 to 1000 km apart. Thus, most of the area falls in the low relief category resulting from a smooth basaltic basement, but is transected by high relief linear features at a spacing of several hundred kilometers.

From the ICSU Ridge to the line of western Pacific trenches at about 145°E, the topography is similar, but with an increased number of seamounts. The Northwest Pacific Basin is predominantly an area of low relief, disrupted only by the Shatsky Rise. To the south, however, there is considerable high relief associated with seamount and island chains, principally the Marshall, Gilbert, and Caroline groups. In this region, one must be especially aware of the differences between Plate II and a bathymetric map. The size of the squares used is larger than the areal extent of most seamounts, thus, the actual area covered by seamounts is much less than that depicted as areas of high relief. On the other hand, as a result of the sometimes sparse bathymetric coverage, not all seamounts have been mapped. Seamounts do, however, show a marked tendency to group rather than occur as isolated individuals. The net result is that Plates I and II delineate areas where there is a high probability of relief in excess of 1900 m.

There is no obvious explanation for the increased number of seamounts in this region. The Marshall-Gilbert chain has been attributed to a hotspot origin. The Line Islands which parallel them, however, have been demonstrated to be of approximately synchronous origin, not time-transgressive as required by hotspot theory. The Mid-Pacific Mountains and the Caroline group are not linear trends. These features all lie on the older half of the Pacific Plate (older than 100 mybp), and their origin can only be speculated upon at the present time. Age data are still too sparse and too uncertain to even state the age of these features relative to the crust upon which they stand. The significant point is: this region was previously viewed as highly abnormal crust because of the scattering of seamounts; it is now considered to be normal crust with an increased number of seamounts, the origins of which have not been determined.

The region to the west (west of 145°E) is a complex region of island arcs and trenches where the rapidly spreading Pacific Plate is being subducted below the Asiatic-Indonesian-Australian continental mass. This region is dominated by high relief, and the low relief associated with the small basins contained within the region will have to be dealt with individually.

Areas of high relief in Plates I and II are areas where significant blockage to acoustic propagation, or major bearing and range errors to the bottom bounce paths will occur. The areas of intermediate relief would tend more to cause localized bearing and range errors, and disruption of convergence paths. Many of the features in this category are too small to be individually mapped, or even detected by the sparse bathymetric coverage in many areas. In the North Pacific Ocean, this scale of relief represents a fringing zone of gradation from the high relief features (seamounts and fracture zones) to the low relief normal crust. In the North Atlantic Ocean, however, this scale of relief is representative of a significant percentage of the basin and results from fracture zones and the corrugated structure of normal crust in areas where sediment cover is thin.

Much of the relief in the low relief category is beyond the mapping ability of all but the highest density bathymetric surveys. This can presently be accomplished in some areas utilizing existing data, but implementation of the necessary surveys to extend the coverage could be justified only by the highest of priorities. Since this scale of roughness virtually spans the range of feature

sizes relevant to low frequency acoustic scattering, an alternative approach to blanket survey coverage must be developed.

#### IV. STATISTICAL APPROACH TO TOPOGRAPHY

Most studies of sea floor topography have been made for geological purposes, and are of a qualitative nature. The few quantitative studies have generally treated the sea floor as though it were a stochastic process, and computed statistical parameters in an attempt to classify morphology. These attempts can be divided into two basic approaches, which are to: (1) estimate the probability density function of depth or slope, or (2) estimate the power spectrum of depth or slope. It should be pointed out that if the sea floor is to be treated as a random spatial series (i.e., noise), the two statistics just mentioned are mutually independent. Middleton (1946) observed that the consequence of the statistical character of noise is that no relationship exists between the distribution of instantaneous amplitudes and the spectral distribution of noise power. Therefore, the power spectrum implies nothing as to the probability of instantaneous depths (or slopes) of the spatial series, or vice versa. This dilemma is further addressed by Helstrom (1968) in the following passage: "Measurement alone cannot establish the collection of probability density functions needed for a complete description of a stochastic process. The expected values, the first-order distribution, and the autocovariance function are usually the only statistical parameters of a process that are practically measurable, and even these can be determined only over limited ranges. As we mentioned earlier, one must have recourse to a model of the process for guidance in setting up a hypothetical class of probability distributions, whose parameters can then be evaluated from what measurements are available."

The most fundamental property that must be established in statistical studies of noise is whether the stochastic process in question is stationary or nonstationary. The conclusion of Krause et al. (1973) was that depths and slopes of the Eastern Pacific sea floor tend to be normally distributed. Exceptions, however, were noted when features such as seamounts or fracture zones were included in the sample "windows", causing skewed or bimodal distributions. Holcombe (1972) found similar results for North Atlantic bottom slopes, where few seamounts exist. In terms of power spectra, Berkson (1975) shows a wide variety of spectral estimates for various physiographic provinces of the North Atlantic Ocean. The implication of these studies is that the statistics of sea floor topography are not constant for all sample windows in all geographic (or physiographic) regions, and sea floor topography, in general, must be considered as a nonstationary stochastic process.

Of the two approaches to quantitative classification of sea floor topography, most investigators have resorted to the power spectrum as their principal statistic, and have followed the convention of the communication theory community by approximating the power spectrum with an exponential function of the form:

$$P(k) = ck^{-n} \quad (3)$$

where  $P(k)$  is the power spectrum in the wave number domain,  $k$  is the wave number,  $c$  is the constant of proportionality, and  $n$  is a constant which characterizes the power spectrum (i.e., white noise, brown noise, etc.).

Nye (1973) has used a dimensional argument to demonstrate that for  $n=3$  the units of power spectrum (meters cubed) cancel, and the power spectrum becomes dimensionless. He has further proposed that  $n=3$  is in fact the value of the power

spectral slope, while Marsh (1964) found  $n=0$ . Although the value of  $n$  is known to vary, when a large number of power spectra are averaged (Bell, 1975) a rather consistent pattern seems to emerge with  $n=2$ . Because the sea floor is quite possibly a nonstationary spatial series, these generalizations could be quite misleading. In terms of Marsh's (1964) theory, an exponent of zero (white noise) would yield a scattering strength varying as the cube of frequency, while an exponent of three would yield a scattering strength independent of frequency.

One characteristic all sea floor power spectra do have in common is a rather consistent fit to an exponential function of the form stated in Equation (3). This is true for virtually all scales of topography, and demonstrates that no matter what the feature size, power is concentrated in the long wavelengths. This, in essence, indicates a lack of features which are tall relative to their horizontal dimension. Features of such a shape would tend to be unstable and short-lived in the ocean environment. At the same time, in the presence of the earth's gravity field, all material tends to migrate down-slope whether the material is sand grains or lava flows. In fact, the work of Menard (1964) and Engle et al. (1965) show that  $15^\circ$  is probably the upper limit for regional slopes of basalt flows forming seamounts and abyssal hills. This would seem to imply that minimization of slope is a dominant factor in sea-floor feature formation. Investigators such as Jacques (1975) have computed the power spectrum of bottom slope rather than depth, and Holcombe (1972) presented slope distribution curves. The slope power spectrum can be obtained directly from the power spectrum of depth. If  $f(x)$  represents a spatial series, then the square of the absolute value of its Fourier transform is, by definition, its power spectrum. This can in turn be approximated by an exponential function.

$$P(k) = |\mathcal{F}[f(x)]|^2 = ck^{-n} \quad (4)$$

Using the identity from Fourier transform theory

$$\mathcal{F}[f'(x)] = jk\mathcal{F}[f(x)] \quad (5)$$

The power spectrum of slope is:

$$S(k) = 2\pi k P(k) = 2\pi ck^{1-n} \quad (6)$$

This simple relationship in itself has implications. If the exponent ( $n$ ) has a value of  $n < 1$ , then the power spectrum of slope will have a positive exponent indicating a power concentration toward the steeper slopes. This case may be theoretically possible, but seems intuitively improbable. A totally unrealistic function such as a Dirac delta function would yield a spectral exponent of  $n=0$ , which is the same as that of white noise, and must be the absolute limiting case. Thus, sea-floor topography can generally be thought of as correlated or "colored" noise, i.e., with a spectral slope in excess of white noise, and probably in excess of the commonly referred to  $1/f$  noise (where  $n=1$ ) of acoustics (Voss and Clarke, 1978).

An additional statistic often used in the theoretical treatment of scattering from rough surfaces is the RMS roughness, or standard deviation of depth around the mean. Although the probability density function cannot be related directly to the

power spectrum, the RMS roughness can. If  $P(k)$  is a power spectrum of the form  $ck^{-n}$  and RMS is the root-mean-square roughness, then,

$$\begin{aligned} \text{RMS} &= \frac{1}{k_2 - k_1} \int_{k_1}^{k_2} P(k) dk = \frac{c}{(k_2 - k_1)(1-n)} [k_2^{1-n} - k_1^{1-n}], n \neq 1 \quad (7) \\ &= \frac{c}{k_2 - k_1} \ln \left( \frac{k_2}{k_1} \right), n = 1 \end{aligned}$$

The RMS roughness can thus be determined for any desired range of wave numbers, and if  $k_1$  and  $k_2$  represent the limits of analysis resolution, the RMS value computed is the standard deviation of depth about the mean depth over the observation window. The same procedure can be applied to Equation (6) to determine a band-limited estimate of the RMS slope.

At this point, it should perhaps be noted that a further implication of Equation (6) is the concept of apparently random sea floor slopes with a continuous spectrum. This is at variance with the simplistic view of monotonically changing depth, i. e., a single slope which persists over considerable distance, which would apply to only continental margins at best. This statistical approach to slope gives rise to a view of the sea floor as being more of a faceted surface, where a received acoustic signal may consist of a number of relatively "coherent" individual returns, each from a separate facet. This would also significantly alter a simplistic view of bearing and range error for single bounce sonar systems.

#### A. BASALTIC RELIEF

Plates I and II indicate that the basaltic crust (in areas free of seamounts and fracture zones) of the North Atlantic is significantly different in character from that of the North Pacific. The North Atlantic basalt is characterized by intermediate scale relief (1100-1900 m relief per 56 km square), whereas the North Pacific basaltic surface is characterized by relief of less than 1100 m. In order to investigate this phenomena, several hundred power spectrums of depth were computed for the basaltic surface in a variety of locations in both the North Atlantic and North Pacific Oceans. These analyses were based upon seismic reflection profiles and bathymetry in areas of little or no sediment cover. The analysis also included a wide variety of sample window lengths that essentially covered the range applicable to wavelengths from a few kilometers to a few hundred kilometers. The resultant spectra were then fitted, in a least squares sense, by Equation (3). A tabulation of the results yielded a consistent exponent ( $n$ ) of 1.76, with a standard deviation of only 0.07. This is not inconsistent with Bell (1975), who found the slope of North Pacific abyssal hill power spectra changed from a value of 2.0-2.5 for wavelengths shorter than a few tens of kilometers to a lower valued exponent for the longer wavelengths.

Bell showed a large apparent scatter with only a few data points in this long wavelength range. The results of the present study included much more data for these wavelengths, but were obtained in a somewhat different manner, i.e., power spectra were computed and fitted by the exponential approximation, then the individual spectral slopes were averaged. This technique was chosen to show the consistency of the gross character of the power spectra in this wavelength range, but does not explain the details of individual spectral estimates. It should be

noted that the mean of the individual standard errors resulting from fitting the exponential approximation to power spectra was 0.35, which is a data scatter comparable to that found by Bell (1975).

These results indicate that within this limited wavelength range, a reasonably consistent relationship between the relative amplitudes of various wave lengths of topography exists for both the North Atlantic and North Pacific Oceans. However, the absolute amplitude associated with a given wavelength is not so easily dealt with. The North Atlantic basaltic surface is dissected by fracture zones that are much more closely spaced than those in the North Pacific. Pacific fracture zones have an average spacing on the order of several hundreds to one thousand kilometers. An analysis of North Atlantic fracture zone spacing for this study yielded an average spacing of only 59.7 km, with a standard deviation of 12.8 km. Holcombe (1972) tabulated the amplitude and wavelength of topography in the North Atlantic. In that study he divided the relief into two categories, a low amplitude short wavelength component, superimposed upon a longer wavelength higher amplitude component. He thus tabulated what he termed local and regional components of relief. The amplitude and wavelengths of his regional component are well within the just-stated range of fracture zone spacing. It is therefore possible that this fracture zone spacing, which is also approximately equal to the grid size of Plate I (56 km), partially accounts for the characterization of the Atlantic basaltic surface by intermediate scale relief. This relief is not so much the result of depth differences associated with the age discontinuities across fracture zones, but results from the second order tectonic deformation associated with the fracture zones. The implication is that the bulk of bathymetric and seismic track data stored in the various governmental and institutional archives can seldom be expected to be free of the influence of fracture zone topography in the North Atlantic. On the other hand, the influence of including these fracture zones does not appear to significantly alter the overall character of depth power spectra from those found for Pacific areas free of this fracture zone influence. Average numbers are usually of limited value, but estimates of RMS roughness for the basaltic basement of the two oceans in the wavelength range from 5 to 100 km is estimated at:  $259 \pm 74$  m for the North Atlantic and  $99 \pm 36$  m for the North Pacific Oceans. This analysis excluded the large fracture zones of the Pacific Basin. The uncertainty indicated is one standard deviation of the individual estimates. The means are significantly different with the North Atlantic having the expected higher value.

In the Holcombe study, which was restricted to the North Atlantic, the mean relief was also determined. This was accomplished by hand tabulation of peak-to-valley heights (peak-to-peak amplitude) and averaging, while the present study computed RMS relief from digitized data. The two cannot be analytically related, but an approximate comparison can be made by assuming the topography to be a sinusoid. This approximation allows the conversion of the "peak-to-peak" amplitude (Holcombe study) to the RMS value, which yielded  $244 \pm 60$  m. The value is in remarkable agreement with the present study. Holcombe also noted that the amplitude of mean relief of the basaltic surface varied from region to region. He essentially found bands of relief paralleling and symmetric about the Mid-Atlantic Ridge, where the mean relief changed from one band to the next, often rather abruptly. He further demonstrated that zones of high mean relief correlated with periods of high orogenic activity in North America and times of slow sea-floor spreading. More recent sea-floor spreading rate estimates, however (Tucholke and Vogt, 1979), do not correlate as well. Luyendyk (1970), on the other hand, suggested that changes in the depth to the magma chambers producing the ridge crest lavas may have determined the amplitude of relief noted in the Holcombe study. Menard (1964) had previously suggested the correlation of basaltic relief with

sea-floor spreading rates, but never attempted to quantitatively verify the relationship.

It has been shown in this study that the North Atlantic has significantly higher mean relief on the basalt than the North Pacific in areas free of seamounts and large fracture zones. The Atlantic also has much slower average spreading rates than the Pacific (2-4 cm/yr versus 6-16 cm/yr total spreading rates). To test the spreading rate versus basaltic relief hypothesis, data were carefully chosen from only the Pacific Ocean. The Pacific has an adequate span of spreading rates, and possible inherent differences between oceans would be excluded. In any study of this nature, there is always the question as to how to select the data to be used. In this case it was decided to: (1) use only bathymetric data in areas of minimal sediment cover to reduce depth errors inherent to seismic reflection data (see Appendix C), (2) to use only carefully selected profiles free of seamounts and fracture zones, and (3) to use areas where only the best available spreading rate control existed (Handschumacher, 1976). These three constraints reduced the available data base to the point where only a few valid data points exist, a summary of which is presented in Table 1.

Table 1  
Spreading Rate Versus RMS Relief for Selected Profiles  
of the Basaltic Basement in the Pacific Ocean

<u>RIDGE</u>	<u>MAGNETIC ANOMALY WINDOW</u>	<u>TOTAL SPREADING RATE (cm/yr)</u>	<u>RMS RELIEF (meters)</u>	<u>MEAN RMS RELIEF (meters)</u>
Nazca-Cocos	0-2'	6	104	108
Chile	0-3'	6	111	
Chile	3-5'	10	48	
Pacific-Antarctic	0-3'	10	91	
Chile	3-5'	10	106	
Pacific-Antarctic	0-3'	10	135	130
Pacific-Antarctic	0-3'	10	153	
Chile	3-5'	10	176	
Pacific-Antarctic	0-3'	10	204	
Nazca-Pacific	0-2'	16	102	
Nazca-Pacific	0-2'	16	164	133

It appears from these results that no consistent pattern exists between sea-floor spreading rate and RMS relief of the basaltic surface in the spreading rate range of 6-16 cm/yr in the Pacific Ocean. This does not, however, preclude the possibility that there may be a spreading rate threshold below which mechanisms change, resulting in a sudden change in basaltic relief.

Holcombe (1972) pointed out that the apparent bands of relief paralleling the spreading axis were symmetric about the axis. No ready explanation of these bands is available; however, the existence of such sudden shifts in relief amplitude

was verified. In an area of the Atlantic bounded by 26°-31°N and 22°-27°W, a seismic reflection survey was conducted in 1971 which consisted of 33 east-west parallel lines with an average spacing of 17 km. Visual observation showed a distinct boundary between "rough" and "smooth" basaltic basement where the approximate crustal age is 105 mybp (Albian or uppermost Lower Cretaceous Age). Computation of mean RMS relief for the two areas yielded 292 and 136 m, respectively. The slopes of the power spectra for the two regions, however, were virtually identical. Such shifts in basement RMS relief undoubtedly exist in the North Atlantic, but have not to date been identified in the Pacific by this or previous studies. Their existence in the Pacific, however, cannot yet be ruled out.

It should also be noted that during the previously discussed analysis of power spectral slopes and RMS relief in the 5-100 km wavelength range, the probability density function (PDF) of depth was also tabulated. The PDF of all samples free of seamounts and fracture zones were found to have a distinct, generally symmetric, central tendency closely approximating a Gaussian distribution. This is in agreement with the findings of Krause et al. (1973) for the North Pacific Ocean, and Holcombe (1972) for the North Atlantic Ocean. Slope distributions were neither computed nor studied in this investigation. It should be recalled, however, that the slope power spectrum can be computed from the depth power spectrum, and would therefore have a spectral slope of 0.76 for this wavelength range.

One further point that should be noted is the possible change in roughness or slope with bearing. All profiles analyzed in this study were chosen perpendicular to the orientation of the magnetic reversal pattern (i.e., parallel to spreading at the time of origin). Larson and Spiess (1970) noted systematic changes in bottom slope distributions with bearing on the crest and flanks of the East Pacific Rise. This is quite reasonable, since abyssal hills have been demonstrated to be elongate in a direction parallel to the ridge crest. Thus, profiles measured perpendicular to the direction of elongation would produce maximum slopes and minimum feature wavelengths, while RMS roughness would be independent of bearing. These variations should be anticipated, but have not been pursued in the present study.

Plate tectonic theory cannot yet explain most of the details of sea floor morphology, but provides an excellent background for speculation. The overall sinuous configuration of the Mid-Atlantic Ridge is thought to result from the breakup of the original mega-continent (Europe, Africa, North and South America). For this sinuous spreading axis to conform to the east-west North Atlantic spreading required by mantle convection, the ridge would have to consist of a number of small segments, which is, in fact, the observed situation. The Pacific spreading ridge, on the other hand, may not have been so originally constrained. Periodic large transform faults are all that is necessary to allow the Pacific plate to conform to the surface of a spherical earth. Proximity of the Juan de Fuca Ridge to the North American Continent, however, appears to have produced a more fractured, slower spreading ridge somewhat analogous to the Mid-Atlantic Ridge.

The basaltic layer is created at the spreading center by volcanic intrusion and extrusion in the uplifted and tensional environment produced by mantle convection. If the sea floor were to spread at a constant rate with a balanced constant flow of lava to fill the void, there would be no mechanism for producing the elongate ridges commonly termed abyssal hills. If, on the other hand, the spreading is intermittent, the supply of lava irregular, or the two rates act independently, a mechanism is available to form abyssal hills. Although global scale crustal stresses caused by mantle convection can be reasonably assumed to have long-term stability, it would be hard to rule out short-term irregularities of

spreading rates and lava supplies. Luyendyk (1970) has proposed a volcanic model for basaltic emplacement in the Pacific, whereby swarms of dikes near the ridge crest culminating in sills or domed extrusive "piles" produce layer two. He has also pointed out that irregularities of the abovementioned spreading and flow rates would tend to produce irregularities of abyssal hill wavelengths. In his specific study area, faulting long after lava emplacement, possibly related to plate reorientation, also produced a "new" abyssal hill and modified the shape of an existing one. The area of Luyendyk's study was near the Murray Fracture Zone and the California continental margin, an area of oceanic plate which would be expected to contain evidence of tectonic deformation related to subduction of a portion of the East Pacific Rise. Other studies (Spiess et al., 1969) show Pacific abyssal hills of purely volcanic origin in areas where there is no evidence of plate reorientational deformation.

Studies show that the Mid-Atlantic Ridge commonly has a central valley which is not generally present in the Pacific system of spreading ridges. The presently accepted explanation of this feature is based upon the classic model studies of the Rhine graben by Cloos (1930, 1932). His modeled arching of moist clay layers produced a flat-floored depression bounded by uplifted margins, an almost exact scale model of what we now know as the rift valley system of the Mid-Atlantic Ridge. Terrestrial equivalents of this valley exist in Iceland and East Africa; the latter constitutes the first geological use of the word rift, the East African Rift. Numbers 4 and 5, volume 88 of the Geological Society of America Bulletin (1977) contain a collection of papers giving the most detailed descriptions available for this mid-ocean rift system. Their consensus is that most lava is emplaced near the center of the rift floor, and subsequently faulted up to the bordering rift mountains (faulted margin of the rift). As the two plates are transported horizontally away from the rift, crustal cooling and shrinkage causes the upper surface to subside, leaving the rift valley and rift mountains elevated on a regional basis. The final result of this rift mechanism is to produce steep faulted scarps which predominantly face inward toward the spreading axis. Several papers in the abovementioned references tabulate the statistics of these faulted scarps, which commonly have slopes in the 60-80° range. Searle and Laughton (1977) show a well-defined mean spacing of 1.9 km between these scarps, a mean height of about 150 m and a range of height essentially between 0 and 400 m. Evidence shows that within the crestal mountains there is a change in vertical motion, and either fault tilting or faulting downthrown away from the ridge axis tends to reduce the faulted relief outside the rift valley. The point is that faulting parallel to and downthrown toward the ridge axis is a significant contributor to basaltic relief in the North Atlantic that previously has not been demonstrated to exist in the North Pacific Ocean.

Not all segments of the Mid-Atlantic Ridge have an identifiable rift valley. In places on the ridge (such as Iceland, where vulcanism is quite prominent), the rift still exists, but appears to be almost filled. Just to the south on the portion named the Reykjanes Ridge, there is no identifiable rift valley. This waxing and waning of the rift valley and its possible correlation with vulcanism suggest that the prominence of faulting parallel to the spreading axis may be controlled by spreading rate or lava supply. As previously pointed out, the Pacific spreading rates are higher than the Atlantic rates, and in places, almost an order of magnitude higher. Since spreading rates are highly variable even within a given ocean, the importance of rift faulting is also probably variable along a given ridge.

Deep-tow and side-scan surveys in the Atlantic do not show faulting orthogonal to the spreading axis, but do show significant oblique faulting in the

vicinity of fracture zones. High density bathymetric surveys utilizing stabilized narrowbeam echo sounders do, however, show an orthogonal pattern of lineations. These lineations do not have the appearance of fracture zones or recent strike slip faults which would truncate features parallel to the spreading axis. They have more of an appearance of a line along which there is an increased number of abyssal hill terminations and strike changes in bathymetric contours. A tabulation of these lineations on the ridge flanks in areas of thin sediment cover yielded an average spacing of 8.2 km with a 3.3 standard deviation for a mid-latitude area of the North Atlantic. No explanation is readily available. Several investigators have reported en echelon structures in the central rift valley or on the ridge crest (where no rift exists), with a length on the order of 20 km (Searle and Laughton, 1977; Shih et al., 1977; Naval Oceanographic Office, 1976). These features are thought to be centers of lava emplacement; if so, accounting for overlap of the en echelon structure, it is conceivable that such a lava emplacement pattern could account for lineations of the above-stated spacing. The origin of these lineations and their geographic distribution, however, are pure speculation.

The smallest scale of roughness on the basaltic surface results from lava flow structure (pillows), and submarine weathering (chemically and mechanically induced disintegration into fragments). These features, because of their size, are on the fringe of relevance to acoustic scattering and are probably of little importance until more pressing problems have been solved. There is, however, no reason to believe that significant variations from place to place or ocean to ocean exist, except for variation with water depth.

#### B. SEDIMENT MODIFICATION TO BASALTIC RELIEF AND SEDIMENT-GENERATED RELIEF

Pelagic lutites tend to form a thin conformal blanket over the basaltic surface. The carbonate oozes and turbidites, however, tend to fill topographic lows. The manner in which these sediments transform the sea floor from a water-basalt interface to a water-sediment interface could be viewed as a mathematical operator. The pelagic lutites, if truly conformal, would represent an all pass network which produces no change in relief. The sediments that fill lows would, on the other hand, act as clipping circuits, truncating at a constant level in the case of turbidites, and at a variable level in the case of ooze. This act of clipping, mathematically speaking, is a non-linear filter operator, and as such, the transfer function varies with input. For this reason sediment modification of relief cannot be simply dealt with analytically. There is also the added factor of purely sedimentary relief, which would appear as noise added by the "sediment filter."

As a first approximation, however, sediments would be expected to have the response of an attenuator. Although the pelagic lutites are conformal, they are never thick, and thicker sediments which produce clipping would reduce the RMS value of relief. Therefore, as sediment thickness increases, roughness amplitude should decrease. An abyssal plain is the limiting case, an infinite attenuation network, except that if seamounts are present and included, the limiting case would never be effectively achieved. A limited test of this concept was conducted by analyzing and comparing the sediment-basalt interface to the overlying water-sediment interface in areas with varying sediment types in the Atlantic and Pacific Oceans. Figure 5 shows these results in graph of sediment thickness versus the normalized change in RMS roughness. The indicated regression line is represented by equation

$$\text{Thickness (in meters)} = (40. \pm 94.) + 760. \text{ RMS} \quad (8)$$

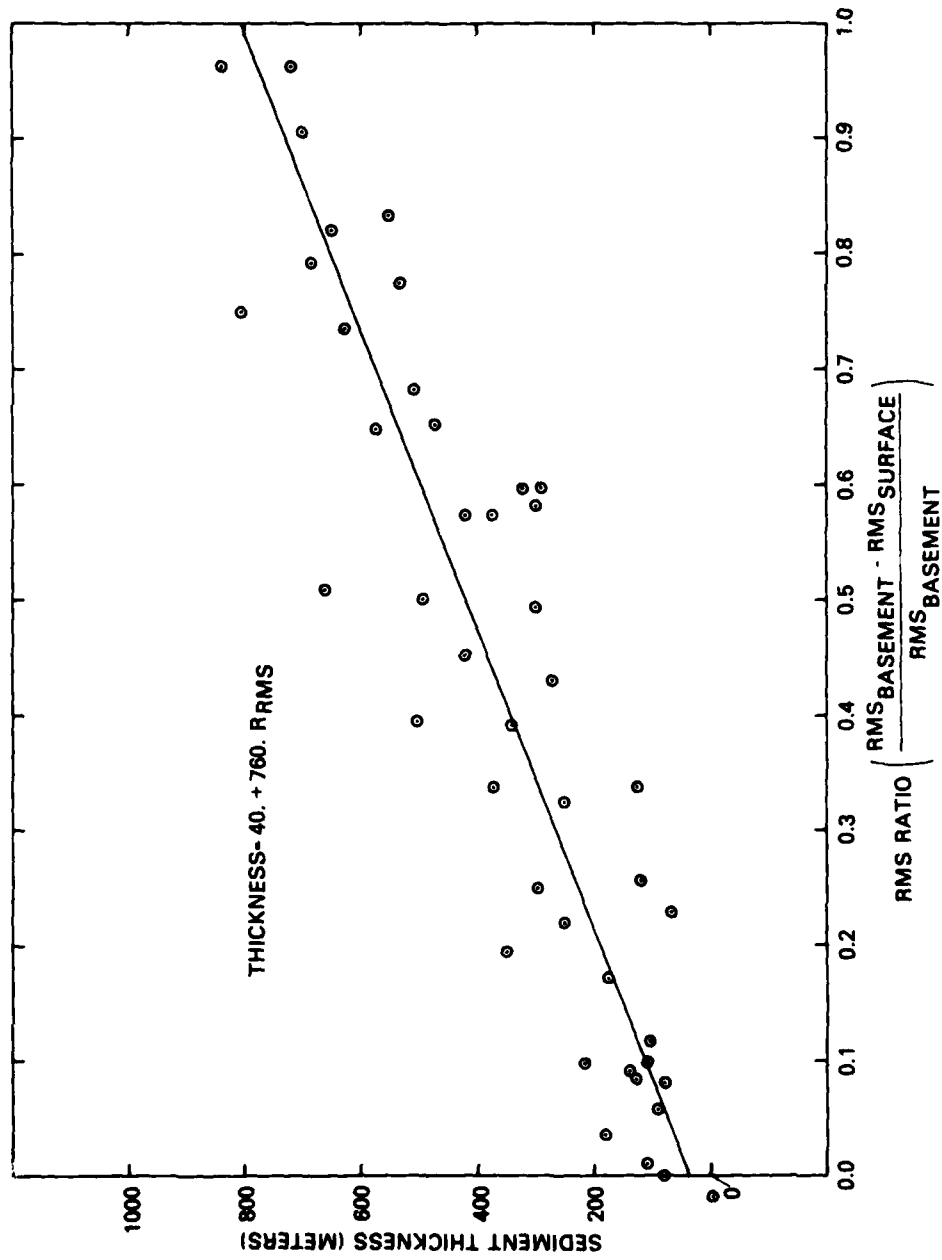


Figure 5. Total sediment thickness versus the ratio of change in RMS roughness to basement RMS roughness.

where  $R_{RMS}$  is the ratio of reduction in RMS roughness to the basement RMS roughness. The standard error of the fit is 94 m. The implication of these results are that: (1) in areas covered by pelagic lutites ("red clays" of the North Pacific), the RMS roughness of basalt is that of the water-sediment interface; and (2) in areas of ooze or turbidite deposition with total sediment thickness less than a kilometer, the basaltic RMS roughness ( $R_B$ ) is

$$R_B = \frac{760 \cdot R_s}{800 - (T \pm 94.)} \quad (9)$$

where  $T$  is sediment thickness in meters, and  $R_s$  is the RMS roughness of the water-sediment interface in meters. The regression error essentially had a Gaussian distribution, thus, the 94 m error bars applied to  $T$  would bound the basement roughness at the 68% confidence level. This analysis is also applicable to the wavelength range of five to one hundred kilometers.

Previous discussion indicated that the power spectrum of the basaltic surface in this wavelength range could be represented by a 1.8 power law exponential function. The same analysis also computed the power spectrum of the water-sediment interface. These computations showed that the two power spectral exponents varied by a mean value of only 0.01. This result, although unexpected, is intuitively in agreement with the nonlinear nature of clipping. For an uncorrelated input such as white noise ( $n = 0$ ), clipping progressively eliminates high negative amplitude spikes, and as such, eliminates high frequency power. For more correlated noise ( $n = 1.8$ ), power is concentrated in the long wavelengths, i.e., the tallest features, and the truncation level of lows must reach a significant percent of the highest relief to alter the power spectrum. Thus, from a practical point of view, the sediment cover essentially acts as a linear filter operator over the limited range of present interest. The transfer function is that of Equation (9) in the feature wavelength range from a few kilometers to one hundred kilometers. This wavelength range is essentially outside the range of most features of purely sedimentary origin.

Further refinement of this approach is not deemed warranted because the effects of bottom currents and post-depositional tectonic deformation produce relief of the same order of magnitude as the error bars on the estimate. This essentially states that the limiting signal-to-noise ratio has been reached. For the same reason, this approach is not applicable to the shorter wavelengths. As wavelengths become shorter, amplitudes become less and the signal is further buried in the noise. Sea-floor morphological forms with amplitudes less than approximately 100 m and wavelengths less than approximately 5 km include features of purely sedimentary origin. If sediment cover is thin, the acoustic effect of these sedimentary features is probably small relative to the effects of the basaltic basement (Spiess et al., 1969). If, on the other hand, sediment cover is thick, then the relief of the water-sediment interface is probably almost entirely due to sedimentary process. Figure 5 shows that for sediment thicknesses greater than about 600 m the basaltic basement has little effect upon the water-sediment interface at even the long wavelengths. Morphological features of sedimentary origin in areas of thick sediment cover, with wavelengths of less than approximately 5 km, have not been adequately studied, and are beyond the scope of the present investigation.

## V. CONCLUSIONS

The sea floor and the lithologic boundaries below it can generally be thought of as interfaces of acoustic impedance mismatch. The significance of these interfaces to low-frequency acoustic propagation varies widely. The high

variability results from a combination of operational factors (such as source-receive geometry or frequency), such environmental factors as the degree of impedance mismatch across the interface, or configuration of the interface itself. The present study addresses the configuration of these interfaces from the environmental point of view. Broad acoustic definitions are used, however, to classify interfaces and sizes of features into general categories according to their acoustic significance.

According to size, there are three basic classes of sea-floor features from the acoustic viewpoint; however, these categories have considerable overlap between them.

1. Large features that block propagation.
2. Intermediate-size features that act primarily as a sloping bottom.
3. Small features that act as scatterers.

If a feature is large enough to completely block propagation, little else matters other than its location. If, however, features allow propagation, but produce sloping and/or rough interfaces, other factors become important. Pelagic sediments are commonly thin, have an acoustic impedance not a great deal higher than sea water and a low acoustic absorption. As a result, the bulk of incident acoustic energy can propagate across the water-sediment interface and through the sediment layer to interact with the sediment-basalt interface. Energy transmitted across the water-sediment interface of thick sediments (such as turbidites) seldom interact with the sediment-basalt interface because of upward refraction resulting from strong positive velocity gradients. Thus, in areas of thin sediment cover, the configuration of the basalt is probably more significant than the sediment surface. In areas of thick sediment, the water-sediment interface configuration is probably more important than the upper basaltic surface.

The largest sea floor features, those which block propagation, are seamounts, fracture zones, and plateaus. The majority of these features in the northern hemisphere have been mapped, and the ones which have not are probably not far removed from trends which have been mapped. To deal with these features in terms of various U.S. Navy systems, it is desirable to have the data in readily accessible digital form. To achieve this, the best available bathymetric maps of the North Atlantic and North Pacific Oceans were collected. This collection included maps from both published literature and unpublished Navy compilations (principally the Naval Oceanographic Office). The maximum, minimum, and mean depths were compiled and digitized for 56 X 56 km squares (30 X 30 vertical mile). This digital data base is available for studies relating to more specific problems. For the present study, however, generalized use is made by first assuming a conservative estimate of propagation blockage as any square having relief in excess of 1900 m. Areas in this category are designated as high relief areas and are depicted in Plates I and II. This depiction showed that the patterns of high relief for the two oceans studied are significantly different. Atlantic high relief is dominated by the crest of the Mid-Atlantic Ridge and the Azores-Gibraltar Ridge. Other areas of high relief are minimal and result from a few island groups and a single seamount chain. Pacific high relief, on the other hand, is dominated by seamounts and large fracture zones.

Relief in the less than 1900 m category also shows distinct differences between the two oceans. A category of topography with relief in the 1100-1900 m range exists in the Atlantic that is virtually nonexistent in the Pacific (see

Plates I and II). In the Pacific, relief is predominantly in excess of 1900 m or less than 1100 m. In the Atlantic there is a small amount of high relief and the remainder is almost equally divided between relief of less than 1100 m and relief between 1100 and 1900 m. This intermediate relief in the Atlantic is associated with an area of thin sediment, and thus reflects relief in the basaltic basement. Most of the North Pacific has sediment thicknesses comparable to this area, but is characterized by low relief, indicating a generally smoother basaltic basement.

The fact that the Atlantic has a rougher basaltic basement than the Pacific (in areas free of seamounts and large feature zones) has been attributed to differences in spreading rates. A test of this hypothesis in the Pacific showed a total lack of correlation between RMS relief and spreading rate for total spreading rates varying between 6 and 16 cm/yr. This does not preclude the existence of a spreading rate threshold below 6 cm/yr, where there is a fundamental change in relief producing mechanisms; however, such a hypothesis has not yet been proposed in the literature. One factor contributing to this difference in relief is the existence of numerous small fracture zones in the Atlantic. An average fracture zone spacing of about 60 km was determined for the North Atlantic, while the North Pacific has a much larger fracture zone spacing of hundreds of kilometers. The result is that almost every square of the Atlantic Relief Map (Plate 1) contains a fracture zone; the associated relief may produce the 1100-1900 m intermediate class of relief that is absent in the Pacific.

To quantitatively study these differences, profiles of the basaltic basement were first digitized from seismic reflection records and bathymetry records in areas of little or no sediment cover. From these profiles, power spectra and probability density functions were computed. Because of beam width considerations, navigational accuracy and sample window lengths, these measurements were band-limited to a wavelength range of a few kilometers to one hundred kilometers. When sample windows were chosen free of seamounts and known fracture zones, a consistent statistical pattern was found. Both oceans appear to have a Gaussian depth-to-basement distribution and a power spectra which can be approximated by wave number to the -1.8 power. The North Atlantic, however, had a mean RMS relief of  $259 \pm 74$  m, while the North Pacific mean was  $99 \pm 36$  m. It appears that the North Atlantic may also have bands of relief paralleling the spreading axis. Estimates of RMS roughness can probably be further refined by producing relief province maps. Pursuit of this venture would, however, be time consuming and the undertaking would depend upon the value of such a study to the applied acoustic community. Such bands of relief have not as yet been identified in the Pacific Ocean.

Once the basaltic crust has formed the spreading axis, an almost continuous accumulation of sediment begins. Different types of sediment accumulate in different manners, some into depressions, others resting as conformal blankets. The manner in which these sediments alter the sea floor from a water-basalt interface to a water-sediment interface thus depends upon the sediment type. An analytic treatment of how these sediments alter topography quickly leads to nonlinear filter theory, which is not deemed warranted. However, since the conformal sediments (pelagic lutites) are always thin and the depression-filling sediments (oozes and turbidites) are usually thicker, an empirical treatment is possible. The filling of depressions reduces the amplitude of relief. Equation (8) presented the linear regression equation relating reduction in RMS relief to mean sediment thickness. This regression equation has a standard error of 94 m indicating the grossness of the estimate, although Figure 5 clearly indicates an approximately linear relationship. Comparing the power spectra of the water-sediment to sediment-basaltic showed no appreciable change in the -1.8 power of wave number. These results occur because longer wavelength features are of higher

amplitude and are the last to be buried, thus requiring appreciable filling before the long wavelength-dominated power spectrum is altered. These data are from the same seismic reflection records used in the study of basement power spectra, and are therefore applicable to the same wavelength range of a few to one hundred kilometers.

The study of features with wavelengths of less than a few kilometers is much more difficult. From a geophysical point of view, measuring the true shape of these features is a major problem. A deep-towed transducer navigated by transponder net is the most accurate means, but the areal coverage is extremely limited. The use of gyro-stabilized, narrowbeam surface transducers with a combination of inertial, hyperbolic, and satellite navigation systems provides an order of magnitude less resolution, but more than an order of magnitude increase in coverage. Broad-beam surface transducers and seismic techniques are essentially inadequate for this scale of resolution.

The approach of the current investigation has been to outline the problem of relief classification, and address the problems which could be dealt with within resources available. The construction of a statistical model of sea floor relief for wavelengths of less than a few kilometers was not attempted in the present study, nor will it be quickly accomplished in the future. It has been pointed out that there are quite likely inherent differences between the North Atlantic and North Pacific basaltic surface in this relief scale. Correlation between relief and spreading rate has not been investigated in this wavelength band. Classification and description of relief of sedimentary origin will probably have to be based upon a province concept. Sedimentary relief provinces would be expected to be a function of sediment type and bottom current regimes. The possible existence of such relief provinces as those found for larger features in the Atlantic must be investigated. A better understanding of the mechanisms of plate tectonics is necessary to determine the validity of extrapolating descriptions to other areas.

Acoustic modeling currently deals with horizontal surfaces with roughness amplitudes comparable to acoustic wavelengths, or with smooth surfaces with range dependent depth (the sloping bottom problem). The surface configurations between these extremes, however, pose a significant computational problem. This is the region where relief is comparable in size to that of the insonified area. A receiver may view several "coherent" returns, each from a different facet of the reflecting surface, similar to the light reflected from the water-air interface in the presence of a light breeze. This intermediate case appears most representative of the sea floor where RMS relief is measured in hundreds of meters. Although such a surface is actually deterministic, its features are generally too small to be individually mapped and must be described statistically.

Before further attempts are made to construct roughness models, the definition of relief scales of importance and lithologic surfaces of interest should be defined. Essentially all topographic measurements are band-limited, thus, the bands of interest must be defined before large-scale investigations are undertaken. The boundaries between rough and smooth, or between rough and sloping, should be defined more precisely. Determination should be made as to when the water-sediment or sediment-basalt surface is of primary interest. These are factors which determine the desired window lengths, resolution, and analysis procedures to be used in relief analysis.

This has been an attempt to outline the problem of the quantitative study of sea-floor topography. A few questions have been answered for the present, and many more have been raised. Although the purpose was to provide information for the

marine acoustic community, the problem had to be approached from an understanding of geologic processes. The blind application of statistical descriptions or extrapolation from one area to another would be a disaster without the guidance of at least a qualitative understanding of sea floor processes.

## VI. REFERENCES

- Be', A. and D. S. Tolderlund (1971). Distribution and Ecology of Living Planktonic Foraminifera in Surface Waters of the Atlantic and Indian Oceans. In: B. M. Funnel and W. R. Riedel (eds.), *Micropaleontology of Oceans*, London, Cambridge Univ. Press., p. 205-221.
- Bechmann, P. and A. Spizzichino (1963). The Scattering of Electromagnetic Waves from Rough Surfaces. MacMillan Co., p. 9-16.
- Bell, T. H. (1975). Topographically Generated Internal Waves in the Open Ocean. *Jour. Geophys. Res.*, v. 80, p. 320-327.
- Berkson, J.M. (1975). Statistical Properties of Ocean Bottom Roughness (Abs.), Power Spectra of Ocean Bottom Roughness. *Jour. Acous. Soc. Amer.*, v. 58 (S1), p. 587.
- Cloos, H. (1930). Zur Experimentellen Tektonik. *Die Naturwissenschaften*, Jhg. 18, p. 714-747.
- Engel, A. E. J., C. G. Engel, and R. C. Havens (1965). Chemical Characteristics of Oceanic Basalts and the Upper Mantle. *Bull. Geol. Soc. Am.*, v. 76, p. 719-734.
- Ewing, M., G. Carpenter, C. Windisch and J. Ewing (1965). Sediment Distribution in the Oceans: the Atlantic. *Geol. Soc. Amer. Bull.*, v. 84, p. 71-88.
- Ewing, J., M. Ewing, T. Aitken, and W. J. Ludwig (1968). North Pacific Sediment Layers Measured by Seismic Reflection. In: *The Crust and Upper Mantle of the Pacific Area*, L. Knopoff, C. L. Drake and P. J. Hart (eds.), *Amer. Geophys. Union Mono. 12*, *Geol. Soc. Amer.* (1977), pp. 174-188.
- Handschumacher, D. W. (1976). Post-Eocene Plate Tectonics of the Eastern Pacific. In: *The Geophysics of the Pacific Ocean Basin and Its Margin*. *Amer. Geophys. Union Mono. 19*, p. 177-204.
- Helstrom, C. W. (1968). *Statistical Theory of Signal Detection*. Pergamon Press, London, p. 45.
- Heezen, B. C. and D. J. Fornari (1975). Geological Map of the Pacific Ocean. In: *Initial Reports of the Deep Sea Drilling Project*, J.E. Andrews and G. Packham et al., v. 30, Washington, DC, back pocket
- Holcombe, T. L. (1972). Roughness Patterns and Sea-floor Morphology in the North Atlantic Ocean. Unpublished Ph.D. Dissertation, Columbia Univ., New York.
- Jacques, A. T. (1975). Bottom Slope Determinations: Differences in Methods. *Jour. Acous. Soc. Am.*, v. 58, Supplement 1, p. 29-30.
- Jones, E. J. W., M. Ewing, J. Ewing and S. L. Eittreim (1970). Influences of Norwegian Sea Overflow Water on Sedimentation in the Northern North Atlantic and Labrador Sea. *Jour. Geophys. Res.*, v. 75, p. 1655-1680.
- Krause, D. C., P. J. Grim, and H. W. Menard (1973). Quantitative Marine Gemorphology of the East Pacific Rise. NOAA Tech. Rept. ERL 275-AOML 10, p. 1-73.

- Kent, D., N. D. Opdyke and M. Ewing (1971). Climate Change in the North Pacific using Ice-Rafted Detritus as a Climatic Indicator. *Geol. Soc. Amer.*, v. 82, p. 2741-2754.
- Larson, R. L. and F. N. Spiess (1970). Slope Distributions of the East Pacific Rise. *Scripps Institution of Oceanography, S.I.O. Publ.* 70-8, p. 1-4.
- Luyendyk, B. P. (1970). Origin and History of Abyssal Hills in the Northwest Pacific Ocean. *Geol. Soc. Amer.*, v. 81, p. 2237-2260.
- Marsh, H. W. (1964). Reflection and Scattering of Sound by the Sea Bottom, Part I. Presented at 68th meeting of the Acous. Soc. Amer., Oct. 1968.
- Menard, H. W. (1964). *Marine Geology of the Pacific*. McGraw Hill Book Co., New York, NY.
- Middleton, D. (1946). The response of Biased, Saturated Linear and Quadratic Rectifiers to Random Noise. *Jour. Appl. Phys.*, v. 17, p. 778-801.
- Morton, W. T. and A. Lowrie (1978). Regional Geological Maps of the Northeast Pacific. Naval Oceanographic Office, NSTL Station, MS., RP-16, p. 16.
- Naval Oceanographic Office (1976). Bathymetric Navigation Chart BNC 0904-224, NSTL Station, MS.
- Nye, J. F. (1973). A Note on the Power Spectra of Sea-ice Profiles. *AIDJEX Bull.*, n. 21, p. 20-21.
- Rayleigh, J. W. S. (1945). *The Theory of Sound*. Dover Publications, Inc., New York, NY.
- Ridley, W. I., N. D. Watkins and D. J. MacFarlane (1974). The Oceanic Islands: Azores. In: A. E. M. Narin and F. G. Stehli (eds.), *The Ocean Basins and Margins*, Vol. 2, Plenum Publishing Corp., p. 445-483.
- Riddihough, R.P. (1978). The Juan de Fuca Plate. *Trans. Amer. Geophys. Union*, v. 59, p. 836-842.
- Ruddiman, W. F. (1977). North Atlantic Ice-rafting: A Major Change at 75,000 Years Before the Present. *Science*, v. 196, p. 1208-1211.
- Searle, R. C. and A. S. Laughton (1977). Sonar Studies of the Mid-Atlantic Ridge and Kurchatov Fracture Zone. *Jour. Geophys. Res.*, v. 82, p. 5313-5328.
- Shih, J.S.F., T. Atwater and M. McNutt (1978). A Near-Bottom Geophysical Traverse of the Reykjanes Ridge. *Earth and Planetary Science Letters*, v. 39, p. 75-83.
- Spiess, F. N., B. Luyendyk, and M. S. Loughridge (1969). Bottom Slope Distributions and Implied Acoustic Bearing Errors in Abyssal Hill Regions of the North Pacific. *Jour. Underwater Acous.*, v. 19, p. 183-196.
- Tucholke, B. E. and P. R. Vogt (1979). *Synthesis of Western North Atlantic Depositional and Tectonic History (In Press)*. Initial Reports of the Deep Sea Drilling Project, v. 43, Washington, D.C. (U.S. Govt. Printing Office).
- Voss, R.F. and J. Clarke (1978). 1/f Noise in Music: Music from 1/f Noise. *Jour. Acous. Soc. Amer.*, v. 63, p. 258 - 263.

APPENDIX A  
ORIGINS OF SEA FLOOR TOPOGRAPHY

## APPENDIX A

### ORIGINS OF SEA FLOOR TOPOGRAPHY

#### FEATURES OF TECTONIC/VOLCANIC ORIGINS

Little was known about sea floor topography until echo sounders became available during the early 1920's. The proliferation of ships equipped with these devices during World War II led to a highly improved definition of the sea floor. By the 1950's, it was known that there were submarine mountain chains, somewhat misleadingly termed ridges, and that these mountain chains formed a world-encircling system. During this same era, the field of paleomagnetism was providing evidence that the continents had moved relative to each other. To account for these phenomena, many marine geologists began reviving and revising earlier concepts of continental drift (Wegener, 1912) and ocean-floor spreading (Holmes, 1931). Additional submarine features such as trenches, fracture zones, seamounts, and guyots were also being found, charted and explained by these emerging theories, which have come to be known collectively as the "new global tectonics," or, plate tectonic theory.

The founding of modern plate tectonic theory is usually attributed to Harry H. Hess (1962). His theory states that the earth's crust is composed of rigid plates which move horizontally as a result of thermal convection deeper within the earth. As the plates are horizontally moved apart at the ridges, basaltic material rises to fill the void. To compensate for this continuous production of new crust, oceanic trenches subduct crust and assimilate it back into the mantle. Thus, the oceanic crust is believed to be continually formed and destroyed, with a near-zero net change in volume. The oldest oceanic crust in existence at the present time is probably in the western Pacific and dates on the order of 200 million years before present (m.y.b.p.). Although many details of crustal formation are not yet known, it is generally accepted in the scientific community that: (1) basaltic material comes up at or near the ridge or rise axis as lava flows, dikes, and sills to form the basaltic layer (seismic layer 2) of the oceanic crust; (2) as new material is emplaced and the crust moves horizontally away from the spreading axis, cooling of the basaltic and lower layers causes the crust to subside, and this subsidence causes the spreading axis area to be topographically elevated relative to the basins, thus forming the "spreading ridge or rise"; and (3) to allow this moving plate system to conform to an approximately spherical earth surface, the ridge system must be offset in places by transform faults which produce the fracture zones extending at right angles to the ridge system. Adjustments to this dynamic plate system can cause later deformation of the solidified crust, and/or volcanism along the fracture zones. In addition, isolated, nonlinear magmatic upwellings of small areal extent are believed to exist, and have been termed "hot spots." The concept of stationary upwellings (hot spots) under a moving plate is used to explain the long linear chains of volcanoes, which grade in age from recently active to long extinct. There are, in addition, island chains, plateaus and other features for which no ready explanation presently exists. For a more thorough discussion of plate tectonic theory in general, the reader is referred to Bird and Isacks (1972) or Cox (1973). The remainder of the discussion here is directed toward more specific aspects of plate theory which have direct bearing upon sea floor topography.

H. W. Menard (1967) has been responsible for postulating plate tectonic explanations for much of the sea floor's morphology. One of these postulations, later quantified in Sclater and Francheteau (1970) and Sclater et al. (1971), demonstrates the effect of crustal cooling and subsequent shrinkage with time after

formation. This effect produces a regional exponential increase in depth to basalt with distance from the spreading axis, until the basaltic basement reaches an approximate age of 40-50 m.y.b.p. Beyond this point, the depth increase is relatively small. The absolute value of this regional slope is thus dependent upon the spreading rate history of the given segment of ridge which produced the area of crust in question. A plot of depth below the ridge crest versus distance from the ridge axis for various spreading rates is shown in Figure 6A. It is apparent from this figure that maximum regional slopes of only  $0.3^\circ$  can be produced by this mechanism. It should be noted that the accumulation of sediment on top of the basalt will cause further subsidence to achieve isostatic equilibrium. The depth adjustment is approximately one-half the total thickness of sediment; this increase in sediment thickness with distance from the ridge produces a net reduction in regional slope of the sea floor, but increases slope on the basaltic surface.

This crustal subsidence phenomenon also produces depth differences across fracture zones. Since fracture zones offset the spreading axis, there is an age difference across fracture zones. The "Sclater" time-depth curve transforms this age differential into an actual depth difference. Thus, the portion of a fracture zone separating crust which is less than 40-50 m.y. old will have a step increase in depth when going from the younger to older plate segment. The magnitude of this discontinuity is a function of absolute age and age difference. Figure 6B plots depth difference across a fracture zone versus age of the younger crust for several age differentials. The maximum known age differential across a fracture zone is approximately 25 m.y. between crustal segments dated at 10 and 35 m.y.b.p. This would predict approximately one kilometer as the maximum relief across a fracture zone.

Relief in excess of one kilometer is, however, commonly found in association with fracture zones, but this is generally attributed to secondary tectonics associated with the fracture zone, not simply age difference. It is also reasonable to assume that a convective system would change with time, and such obstructions as continents, island chains, or plateaus would occasionally be jammed into a subduction zone or override a spreading zone. These anomalous events would require readjustments of plate motion, possibly even on a global scale. Additional questions have been raised as to the effect of translating a crustal plate over the surface of a spheroid (Oxburgh and Turcotte, 1974). Therefore, although crustal cooling explains the relief of spreading axes and fracture zones, the theory has not yet been refined to a predictive model.

Menard (1967) has also suggested that the volume of lava discharged per unit length per unit time from spreading centers was relatively constant regardless of the spreading rate. He also pointed out that: (1) zones of slow spreading (1-2 cm/yr half-rate) were characterized by a central rift valley, adjacent high rift mountains, and a thick basaltic layer, while (2) zones of fast spreading (3-4.5 cm/yr half-rate) were characterized by the absence of a central rift valley, subdued topography, and a thin basaltic layer. If, in fact, the volume of basalt emplaced at the spreading axis is near constant, the thickness and upper surface topography of the basaltic layer of oceanic crust would be a function of spreading rate. Luyendyk (1970) demonstrated that Pacific abyssal hills topography is partially a result of volcanic activity near the spreading rise, and partially from later faulting due to reorientations in plate motion. Studies in the Atlantic (Searle and Laughton, 1977) where spreading is generally slower and a central rift valley exists, indicate that faulting in the rift valley is the dominant cause of abyssal hills in that ocean's topography. These studies indicate that the topography of the "normal" crust, i.e., basaltic surface, between fracture zones and free of seamounts, trenches, etc., consists predominantly of elongate features roughly

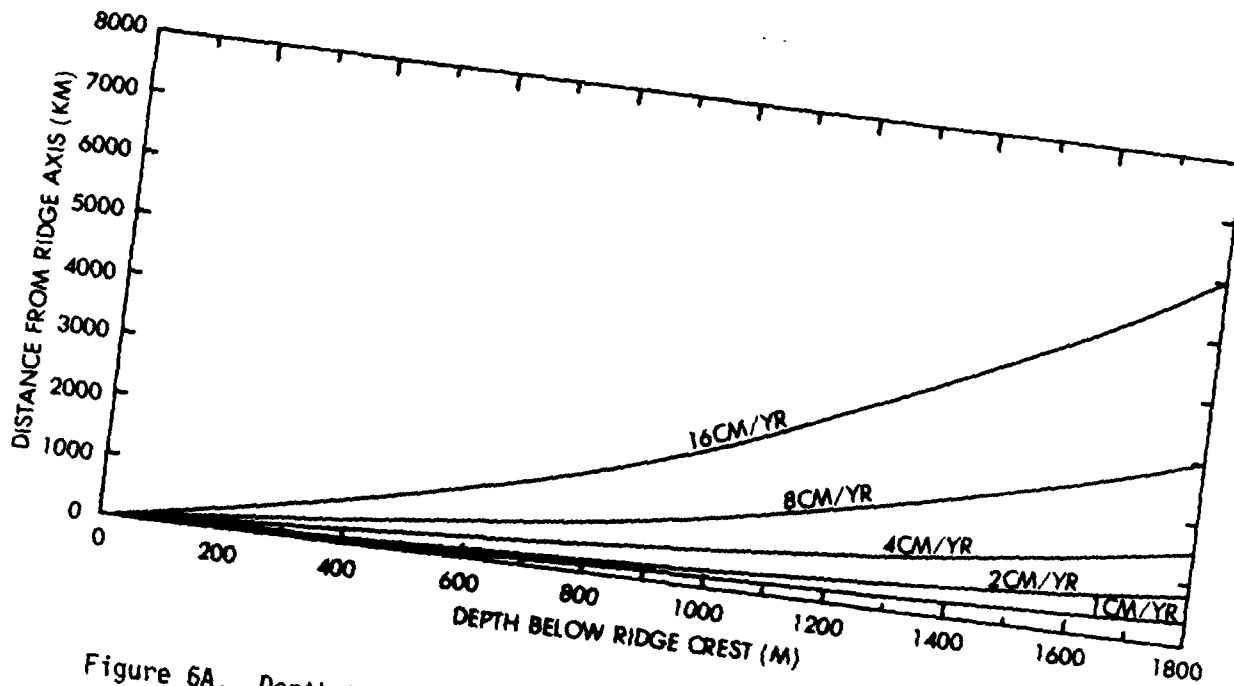


Figure 6A. Depth below the ridge crest of the basaltic surface versus distance from the ridge axis. Individual curves represent different spreading rates.

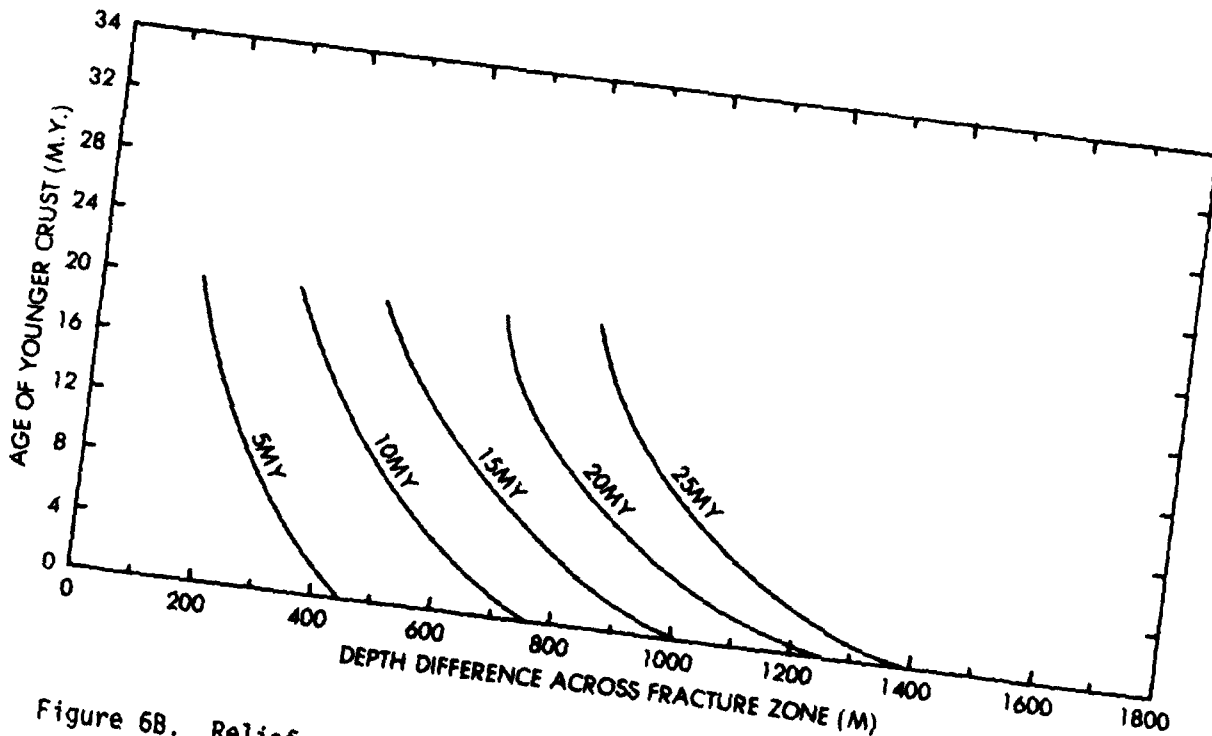


Figure 6B. Relief across a fracture zone versus age of younger plate segment for various age differences across the fracture zone.

parallel to the spreading axis. High resolution bathymetric surveys made with transponder-navigated, deep-towed, narrow-beam echo sounders (Spiess et al., 1969, and Larson, 1972) confirm that basaltic features near the ridge crest and in the subsequent abyssal hills are, in fact, ridges parallel to the spreading axis with lengths on the order of ten times their width. The topographic texture of this normal basaltic crust can therefore be characterized by a series of parallel ridges formed by lava flows and faulting. These ridges are individually discontinuous, but form an overall corrugation pattern parallel to the spreading axis. This current view is somewhat at variance with the term, "abyssal hills," which were originally thought to be more circular in plane view.

Smaller scale features result from the flow characteristics of the basalt prior to cooling, and subsequent "weathering" after cooling. Since the emplacement of basalt at the spreading axis is at a depth of several kilometers, the hydrostatic pressure is sufficient to prevent the dissolved gasses from coming out of solution. This produces a relatively quiet outpouring of lava, as compared to the often explosive eruptions of subaerial volcanics. In addition, the near-zero-degree water, with a thermal conductivity and specific heat higher than that of air, quickly chills and solidifies the outer surface of the basalt. As a result, submarine basaltic lava generally forms in large piles of subspherical or pillow-shaped features which are collectively termed pillow basalts, pillow lavas, or simply, pillow structures. Individual "pillows" range in size from tens of centimeters to meters in diameter. Once the outer shell has hardened into a protective barrier between the molten lava and the chilling sea water, flow within the structure continues, breaking through in places to form new pillows, and often leaves older pillows devoid of lava. Subsequent flows, tectonic activity, and subaqueous "weathering" often break the hollow pillows to form detritus of cobble and boulder size.

#### FEATURES OF SEDIMENTARY ORIGIN

As the crustal plates move, material constantly settles out of the overlying water to form a blanket of sediments over basalt. Where the sea floor is not too deep, calcareous skeletons of planktonic, unicelled animals can rapidly accumulate to form thick sediment covers. In areas where the sea floor is below what is known as the carbonate compensation depth, the calcium carbonate is dissolved by the sea water and the dominant sediment type is "red" clay (lutite), which slowly accumulates from the settlement of atmospheric dust. Near large land masses, terrestrial detritus is periodically redeposited on the deep sea floor by turbidity flows. There are other types of deep sea sediments; however, the carbonate oozes, pelagic lutites and turbidites are by far the predominant types. Of these three types, the first two are deposited relatively conformally over the basaltic surface similar to a "blanket of snow." The cohesiveness of the pelagic lutites tends to hold these sediments in the conformal blanket which is draped over the basaltic basement. The high percentage of sand-sized or silt-sized carbonate grains in the oozes, however, produces a less cohesive sediment, and oozes tend to redeposit in topographic lows as a result of slumping and localized turbidity flows. Like snow, however, the accumulation of these fine sediments is susceptible to currents, and can either be eroded or be swept into thick deposits (one type, a thick sediment lens, is even termed a drift). The spatial distribution of these sediment types depends upon water depth, biological productivity, climatic conditions, proximity to land, and in the case of turbidites, the presence or absence of topographic obstructions (i.e., ridges and trenches) between the source and depositional area. Once deposited, the complex interaction of factors such as depth of burial, temperature, and sediment and pore fluid chemistry work to compact and/or cement the individual sediment grains into a sedimentary rock. Thus, the sea floor topography

is first generated at or near the zones of sea floor spreading, and subsequently is modified by sediment deposition, vulcanism, and tectonic deformation.

As a result, an understanding of plate tectonics and sedimentary processes are vital to studies of sea floor topography. Holcombe (1972) has compiled a definitive analysis of how sedimentation tends to modify the sea floor. His sedimentation model predicts that first, near the spreading ridge, the carbonate sediments tend to settle and concentrate in topographic lows forming "sediment ponds" between the basaltic ridges. As the crust continues to move away from the spreading ridge, subsidence caused by crustal cooling lowers the sea floor below the carbonate compensation depth, and a conformal blanket of pelagic lutite begins to accumulate. As continental margins are approached, the influx of detrital material brought by turbidity flows fills the lowest depressions, and with a sufficient volume of turbidites, abyssal fans and plains will form a relatively smooth sea floor having no correlation at all with the rough basaltic surface beneath.

This progression of sediment types is generally consistent with more recent data from the Deep Sea Drilling Project (DSDP), and is now accepted as the classic deep-ocean sedimentary sequence. There are, however, exceptions. Heezen et al. (1966) first suggested that major sedimentary features are built and shaped by bottom currents which follow the contours of the sea floor (geostrophic contour currents). On a smaller scale, Stanley and Taylor (1977) have presented an excellent description of the unequal distribution of sediment around a seamount that has been subjected to long-term bottom current activity. There are additional factors which tend to alter the classic sedimentary progression, such as blockage of turbidite transport by ridges or trenches, proximity to large rivers, wind patterns, and many more. The majority of these large-scale irregularities, however, have been mapped and logically explained. Smaller features of sedimentary origin also result from fluid movement, but their distributions are less well-known. These are the channels which carry turbidity flows out onto the abyssal plains, sand and mud waves, furrows, and ripple marks. These features range in size from a few centimeters across to several kilometers in width.

#### SYNTHESIS

The topography of a given portion of the sea floor is the composite result of its volcanic, sedimentary, and tectonic history. Figure 7 shows generalized height and width ranges for a number of common sea floor features. Observation confirms intuition in that submarine features, no matter what their origin, are broad relative to their height. It is obvious from this illustration that it is similar to that of Brownian noise.

The basaltic layer forms the primary relief, the larger features of which have been explained in terms of plate tectonic theory. The value of this explanation is that the shape, size, orientation, and position of these features can be extrapolated into areas of poor bathymetric coverage and interpolated between lines for even better definition in reasonably surveyed areas. The fact that the sea floor's basaltic layer has a distinct predictable fabric has been of primary concern to studies of topography. Figure 8 diagrammatically depicts some of these features, and shows how the major sediment types tend to modify or obliterate them. From lower left to upper center is a spreading ridge elevated relative to older crust because of crustal subsidence with age. The central rift valley and high rift mountains are representative only of Atlantic spreading. Laterally through the center is a fracture zone showing younger crust elevated relative to older crust. Superimposed upon the right limb of the fracture zone are two seamounts resulting from later vulcanism. In the upper left is a seamount chain resulting from a hot

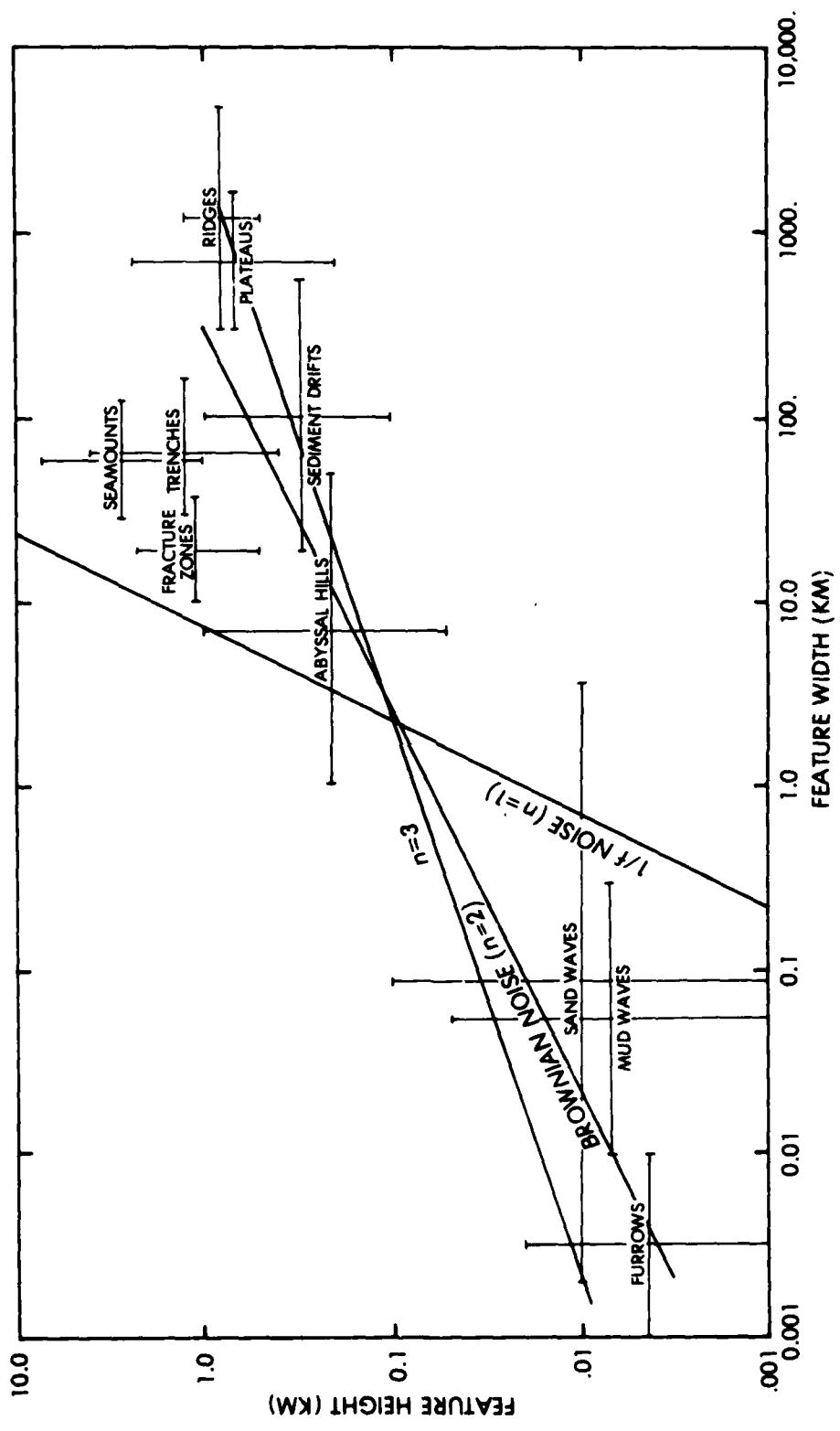


Figure 7. Generalized amplitude and width ranges of common sea floor features. Note the straight line fit of a 1:100 height-to-width ratio which corresponds to a square law power spectrum (Brownian Noise).



Figure 8. Diagrammatic representation of the sea floor showing the major tectonic and sedimentary features.

spot on the ridge flank. These basaltic features are progressively buried with age, first by ponded carbonate sediments, and then followed by a conformal blanket of lutites. The final geologic event depicted is a recent and sudden influx of turbidites covering the right-hand portion of the diagram. It should be noted that the basaltic topography which is exposed on the ridge and protrudes through the sediments on the ridge flanks is depicted as subparallel ridges.

Because of water movement, even on deep ocean floor, some relief features are of purely sedimentary origin and have no relation to the basalt below. Figure 9 shows a seismic section across sand waves which form the Lower Continental Rise Hills province off of the east coast of North America.

Even on the smallest scale, there are flow structures in the basalt as shown in Figure 10. Also note the fine sediment which is ponded into the low relief areas. The ripple marks and ripple defraction patterns around the basaltic obstructions demonstrate the existence of weak abyssal currents, producing relief down to the centimeter scale. The same situation is seen on a larger scale in Figure 11. Here, a seismic reflection record shows the rough basaltic surface still influencing the water-sediment interface, but with the addition of totally independent, current-produced sedimentary features. The best general reference giving a qualitative view of the smaller features of the sea floor is Heezen and Hollister (1971).

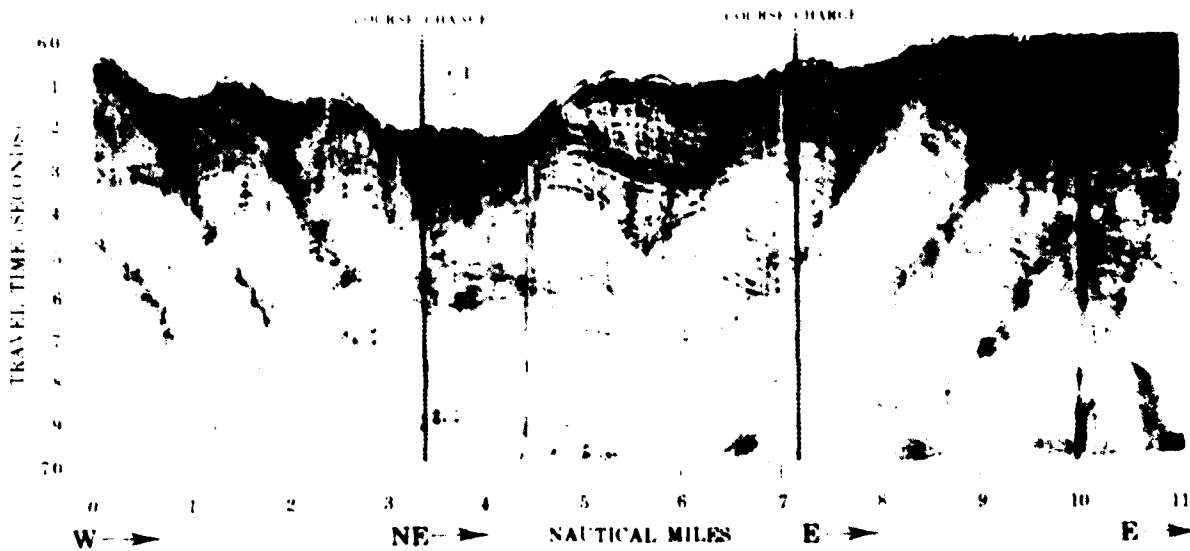


Figure 9. Vertical seismic reflection record of sand waves which comprise the lower Continental Rise Hills off the east coast of North America. In cross section, these marine sand waves are virtually identical to the migrating dunes common to many desert regions.



Figure 10. Deep-sea photograph depicting the top of the basaltic layer with ponded sediments partially covering it. The ripple marks and their diffraction patterns around the outcrops give verification of bottom current activity.

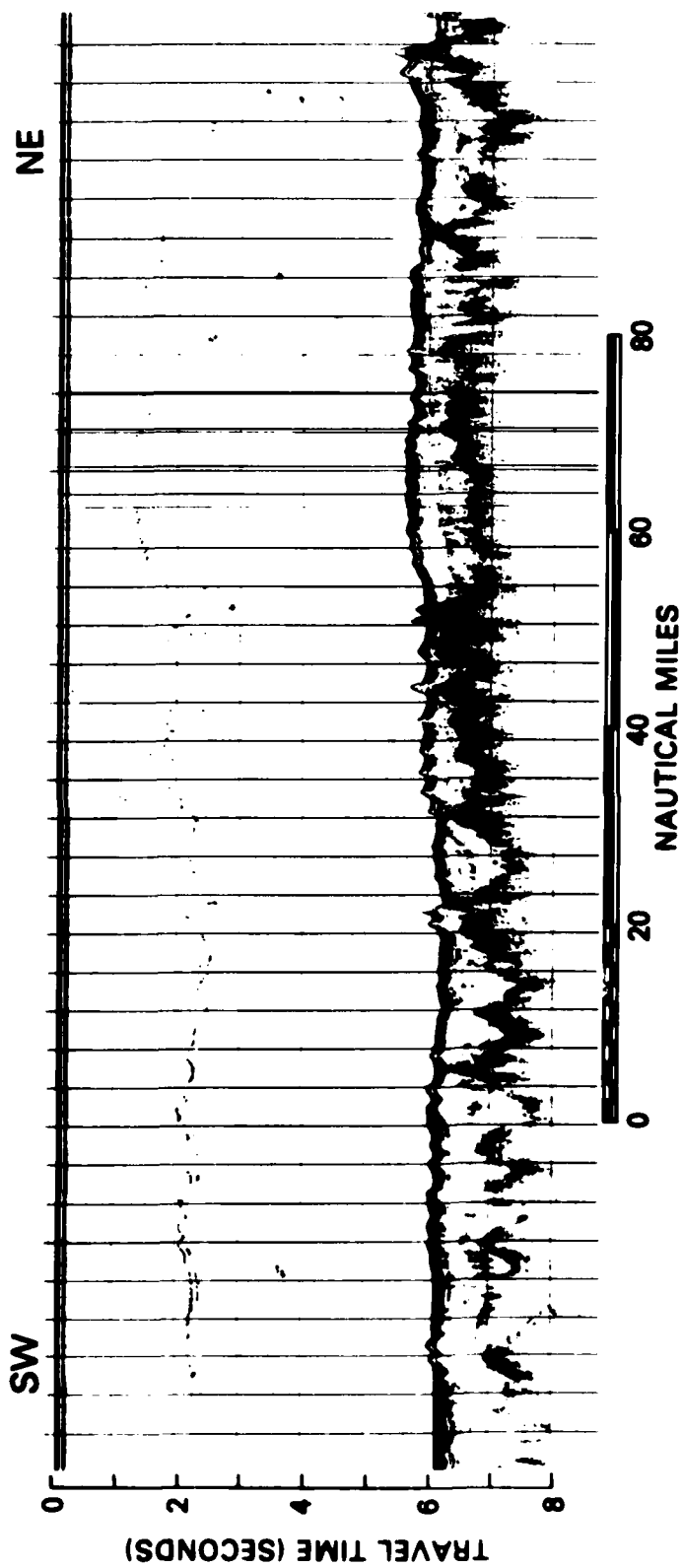


Figure 11. A seismic reflection record showing the typically rough basaltic basement with hemipelagic sediments being deposited. The water sediment interface configuration results from the combination of sediment deposited on a rough surface with bottom current influence.

## REFERENCES

- Bird, J. M. and B. Isacks (1972). Plate Tectonics. Selected Papers from the Journal of Geophysical Research. Amer. Geophys. Union, Washington, DC.
- Cox, A. (1973). Plate Tectonics and Geomagnetic Reversals. W. H. Freeman & Co., San Francisco, CA.
- Heezen, B. C. and C. D. Hollister (1971). The Face of the Deep. Oxford Univ. Press, New York, p. 1-659.
- Heezen, B. C., C. D. Hollister, and W. F. Ruddiman (1966). Shaping of the Continental Rise by Deep Geostrophic Contour Currents. Science, v. 152, p. 1126-1149.
- Hess, H. H. (1962). History of Ocean Basins. In: Petrological Studies: A Volume in Honor of A. F. Buddington, A. E. J. Engle, H. L. James, and B. F. Leonard (eds.), p. 599-620.
- Holcombe, T. L. (1972). Roughness Patterns and Sea-floor Morphology in the North Atlantic Ocean. Unpublished Ph.D. Dissertation, Columbia Univ., New York.
- Holmes, A. (1944). The Machinery of Continental Drift: The Search for a Mechanism. In: Principles of Physical Geology, Thomas Nelson and Sons, Ltd., London.
- Larson, R. L. (1972). Bathymetry, Magnetic Anomalies, and Plate Tectonic History of the Mouth of the Gulf of California. Geol. Soc. Am. Bull., v. 83, p. 3345-3360.
- Luyendyk, B. P. (1970). Origin and History of Abyssal Hills in the Northeast Pacific Ocean. Geol. Soc. Amer. Bull., v. 81, p. 2237-2260.
- Menard, H. W. (1967). Sea Floor Spreading, Topography, and the Second Layer. Science, v. 157, p. 923-924.
- Oxburgh, E. R. and D. L. Turcotte (1974). Membrane Tectonics and the East Africa Rift. Earth and Planet. Sci. Letters, v. 22, p. 133-140.
- Sclater, J. G., R. N. Anderson, and M. L. Bell (1971). Elevation of Ridges and Evolution of the Central Eastern Pacific, Jour. Geophys. Res., v. 76, p. 7888-7915.
- Sclater, J. G. and J. Francheteau (1970). The Implications of Terrestrial Heat Flow Observations on Current Tectonic and Geochemical Models of the Crust and Upper Mantle of the Earth. Geophys. Jour. Royal Astr. Soc., v. 20, p. 509-542.
- Searle, R. C. and A. S. Laughton (1977). Sonar Studies of the Mid-Atlantic Ridge and Kurchatov Fracture Zone. Jour. Geophys. Res., v. 82, p. 5313-5328.
- Spiess, F. N., B. Luyendyk and M. S. Loughridge (1969). Bottom Slope Distributions and Implied Acoustic Bearing Errors in Abyssal Hill Regions of the North Pacific. Jour. Underwater Acous., v. 19, p. 183-196.
- Stanley, D. J. and P. T. Taylor (1977). Sediment Transport Down a Seamount Flank by a Combined Current and Gravity Process. Marine Geol., v. 23, p. 77-88.
- Wegener, A. (1966). The Origin of Continents and Oceans. Dover Publications Inc., New York.

APPENDIX B

DEPTH-DISTANCE ACCURACY  
DEPENDENCE UPON DATA TIME TO  
DISTANCE AND A/D CONVERSION

## APPENDIX B

### DEPTH-DISTANCE ACCURACY DEPENDENCE UPON DATA TIME TO DISTANCE AND A/D CONVERSION

Since the horizontal or "distance" scale of an echogram is time underway, its conversion to actual distance is a function of ship's speed, echo sounder print lines per inch, and echosounder sweep repetition rate. The sweep repetition rate most commonly used is one second for precision depth recorders operated in the deep ocean. The number of sweep lines printed per inch of record paper is usually between 75 and 150, with 100-150 being most commonly used. Ship's speed will generally vary between 5 and 15 kn, with 10 kn as an average. The result is that one inch of fathometer record along the horizontal or distance scale generally represents between 0.26 and 0.76 km of the earth's surface. The major inaccuracy of such a conversion results from navigational error. Errors in navigation cause erroneous estimates of ship's speed of advance (SOA), which could easily be as high as 10% in older data, but is most likely on the order of 1-2% for present-day mid-ocean surveys (utilizing hyperbolic and satellite navigation systems).

Although the commonly referred to sampling theorem by Nyquist states that spectral estimates are valid only up to wavelengths twice as long as the sampling increment, practical experience indicates that the wavelength cutoff ratio is closer to 4-5 times the sample increment. In view of these practical limits, an echogram sampled every 0.2-0.25 in would produce depth spectral estimates valid down to the 0.26-0.76 km wavelength range, dependent upon the factors mentioned above.

Most precision echosounders use 19-inch-wide paper to display one second of two-way acoustic travel time. At an average sound speed in water of 1500 m/s, one inch of record would represent 39.5 m of water depth. Using a nominal 0.05 inch increment to represent the maximum accuracy to which a record can be picked would result in a 2 m depth error, or approximately 0.04% for deep water. Although more accurate picks of the bottom returns could be made, the 0.05 inch error will generally be insignificant in relation to other factors affecting depth error.

If seismic reflection records are the original graphic source of data which are to be digitized, the errors are significantly different. The ship's speed (5-10 kns) and recorded print lines per inch (100-150 lines/inch) are generally the same as for bathymetry; however, the firing rate (equivalent to an echosounder's ping repetition rate) is generally different. Seismic firing rates commonly vary from 4 to 12 seconds. With this firing rate and the same 0.2-0.25 inch digitizing rate, the horizontal or wavelength resolution of seismic data would vary from approximately 0.82 to 9.26 km.

The depth accuracy is also significantly different for subsurface interfaces on seismic records, as opposed to the water-sediment interface on seismic records or echograms. The average vertical speed of sound in the water column of the deep ocean is very near 1500 m/s, and more accurate estimates are easily obtainable. The variation in the velocity of marine sediments and sedimentary material, however, is considerable. Sediment velocity averages computed from measurements made on cores taken by DSDP show a wide variation. Lutites and biogenic oozes usually range from 1500 to 1600 m/s, turbidites from 1550 to 1800 m/s, and limestones and mudstones often range from 1900 to 2500 m/s and higher. The thickness of these layers is also highly variable from a few tens or hundreds of meters for pelagic sediments to several kilometers for sediments of terrigenous origin. Therefore, using the same 0.05 sec picking error as before, depth estimates could easily be in error from 75 to 125 m, even if accurate velocity information is available (approximately

1.5-2.5%). With the scarcity of seismic interval velocity data, these depth error estimates represent minimal values, and absolute depth errors will generally be a percent or two higher.

APPENDIX C  
ERRORS RESULTING FROM BEAMWIDTH

## APPENDIX C

### ERRORS RESULTING FROM BEAMWIDTH

By the early 1930's, publications began appearing which dealt with quantitative interpretations of echograms. These investigations were necessary because echosounders do not measure depth to the sea floor directly beneath them unless the sea floor is perfectly horizontal and smooth. This results from the fact that transducers, or for that matter, any antennas, have a finite transmitting and receiving beam width (i.e., their angular resolution is limited). Hoffman (1957) demonstrated that any sharp projection above the sea floor produces a hyperbolic echo trace. Krause (1962) presented analytic solutions for the echo traces produced by various geometric shapes on the sea floor. Figure 12 illustrates the echogram which would be produced by a sequence of geometrical shapes representing the sea floor based upon Krause (1962). It is obvious from this figure that echosounders produce a distorted view of sea floor topography by causing an apparent increase in feature wavelength and reduction in feature height.

For comparative purposes, both the hypothetical sea floor and the theoretical wide-beam echogram of Figure 12 were digitized, and their power spectral slope and RMS relief computed. The sea floor had a power spectral slope of  $-0.67$  and an RMS relief of 321, while its theoretical wide-beam echogram had values of  $-1.43$  and 181, respectively. This is merely computational confirmation of what is obvious to the eye. The critical factor involved is the ratio of a feature's radius of curvature to the radius of curvature of the echo sounder's wave front. If the wave front radius of curvature is much less than that of the feature, the feature will be reproduced reasonably accurately on the echogram. If, on the other hand, the reverse is true, there will be considerable distortion in the representation of the feature. This distortion is, in essence, a reduction in feature amplitude, and an increase in feature width. For this reason, placement of the transducer closer to the feature to be measured (i.e., deep towed) improves resolution by reducing the wavefront radius of curvature.

Using this wave front radius of curvature criterion and a feature amplitude to wavelength ratio of 1:100 (see Fig. 7, Appendix A), a broad-beam echo sounder will essentially measure features whose wavelength is greater than the depth of water. Therefore, features broader than about 5 km and higher than about 50 m are detected by seismic reflection and broad-beam echo sounders. Echogram distortion is also reduced if a transducer array is used for beam forming, which increases the angular resolution (reduces beam width). Figure 13 shows a comparison of two echograms produced using different beam widths. It should be noted, however, that many narrow-beam echosounders cannot produce a trace on exceptionally steep slopes. This is because the return signal is too far from the vertical to be within the narrow range of angles acceptable to the receiving array.

It is also obvious from Figure 13 that some features on the wide-beam echogram appear to be directly beneath the ship (feature A), but are in fact "side echos", while others of equal definition (feature B) are from features truly beneath the ship. For this reason, it is felt inadvisable to use "educated guesses" when digitizing echograms or seismic records, and preferable to blindly following fixed criterion defining what is considered to constitute the interface of interest. In the current analysis, any echogram feature forming a reasonably continuous trace of features related to the interface of interest was digitized; hence, features A and B in Figure 13 would be digitized as true representations of the sea floor.

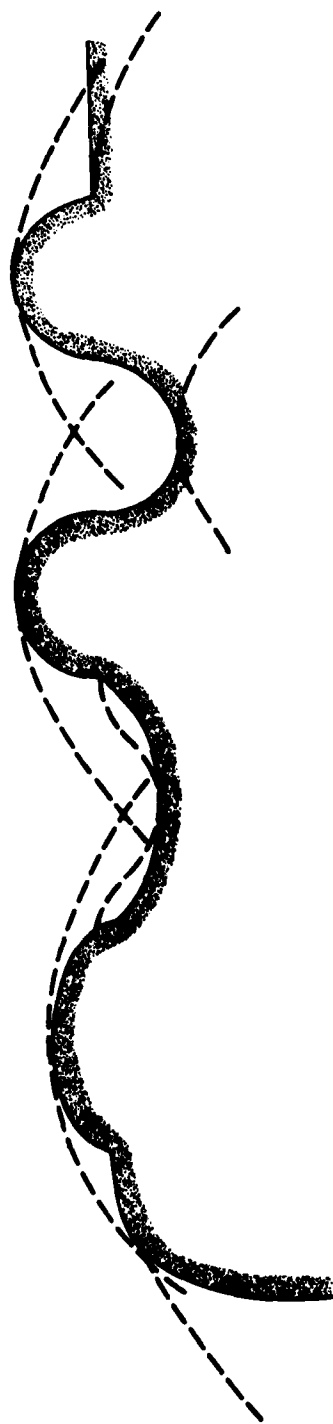


Figure 12. A hypothetical, two-dimensional sea floor composed of geometrical shapes and its associated computed echogram. Constructed from Krause (1962).

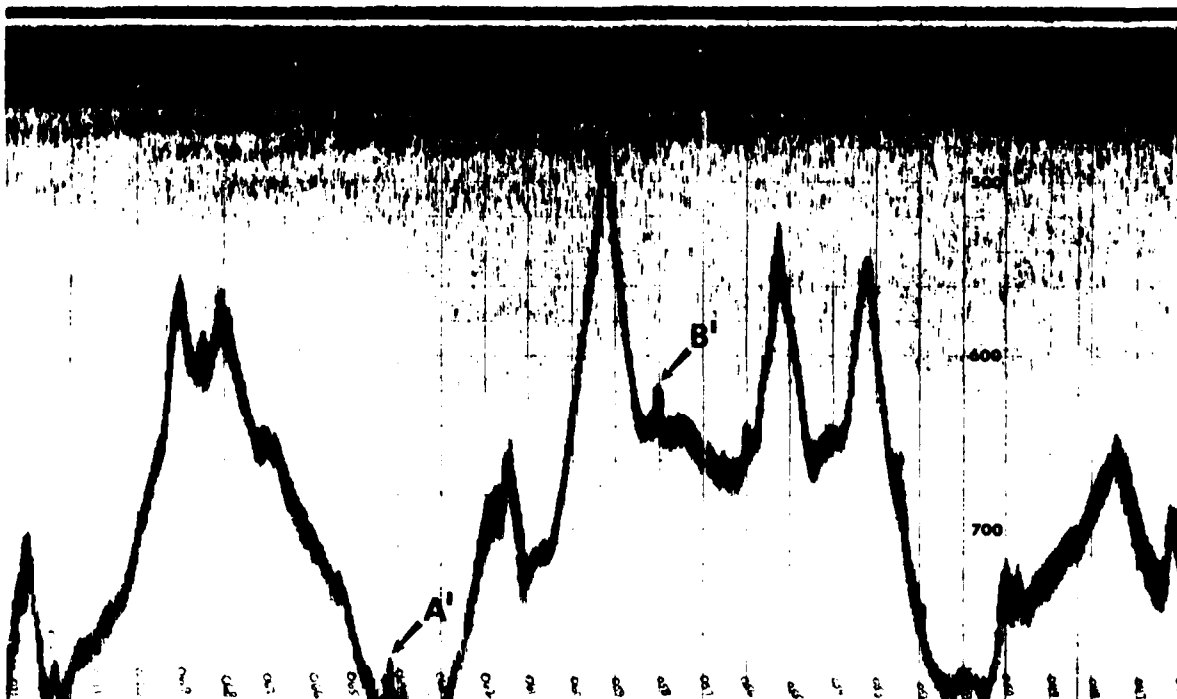
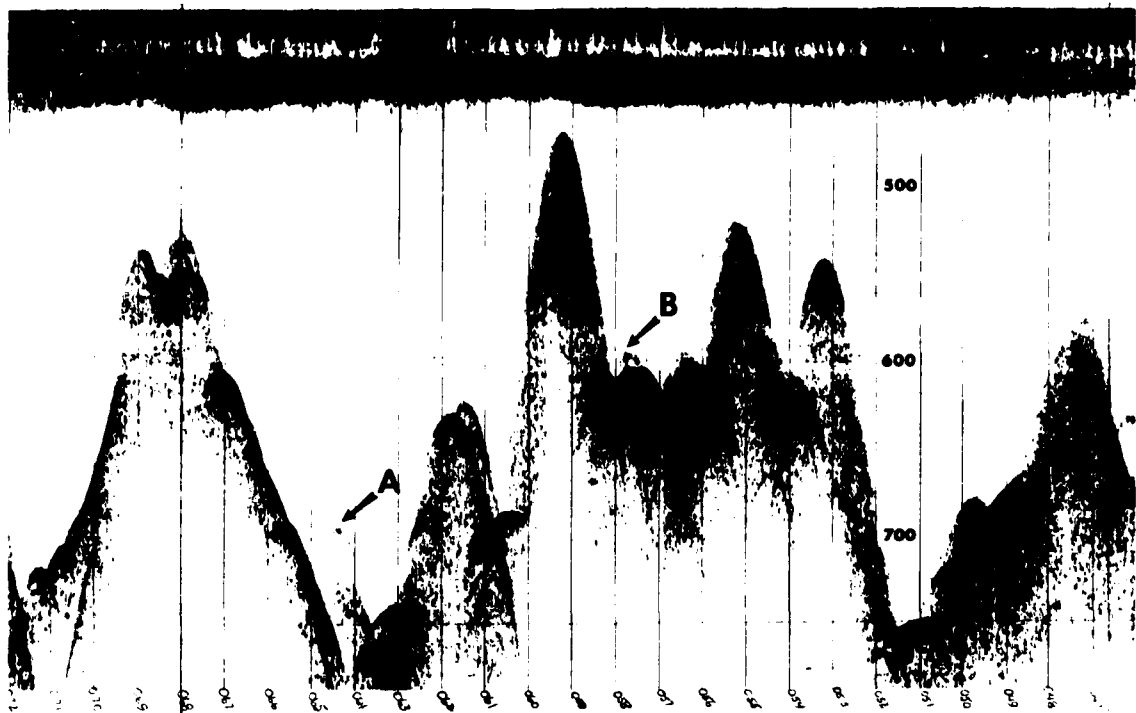


Figure 13. A comparison of wide ( $30^{\circ}$ ) versus narrow ( $2^{\circ}$ ) beam width echo sounders over the same rough bottom.

In the case of seismic reflection records, aside from the wide beam width, the records are further distorted because of the compressional wave velocity structure of the sediment cover. The problem is similar in that oblique arrivals are printed on the record as though they were vertical arrivals. However, the complexity is increased by the fact that the oblique arrivals may have obliquely penetrated several layers of differing velocity and may have been refracted at several interfaces. Their printed position is therefore a function of sediment velocity as well as geometrical position. Slight changes in the thickness of high velocity layers can also significantly change the ray travel time.

REFERENCES

Hoffman, J. (1957). Hyperbolic Curves Applied to Echo Sounding. Int. Hydrographic Rev., v. 34, p. 45-55.

Krause, D. C. (1962). Interpretation of Echo Sounding Profiles. Int. Hydrographic Rev., v. 39, p. 65-123.

Unclassified

9) Technical report

SECURITY CLASSIFICATION OF THIS PAGE (When Data Entered)

REPORT DOCUMENTATION PAGE		READ INSTRUCTIONS BEFORE COMPLETING FORM
1. REPORT NUMBER NORDA Technical Note 47 /	2. GOVT ACCESSION NO. HD-4093702	3. RECIPIENT'S CATALOG NUMBER
4. TITLE (and Subtitle) 6) An Approach to the Quantitative Study of Sea Floor Topography		5. TYPE OF REPORT & PERIOD COVERED
7. AUTHOR(s) 10) J. E. Matthews		8. CONTRACT OR GRANT NUMBER(s) 14) NORDA-TN-47
9. PERFORMING ORGANIZATION NAME AND ADDRESS Naval Ocean Research and Development Activity / NSTL Station, Mississippi 39529		10. PROGRAM ELEMENT, PROJECT, TASK AREA & WORK UNIT NUMBERS 17441
11. CONTROLLING OFFICE NAME AND ADDRESS Sea Floor Division Naval Ocean Research and Development Activity NSTL Station, Mississippi 39529		12. REPORT DATE 17 Jan 1980
14. MONITORING AGENCY NAME & ADDRESS (if different from Controlling Office)		13. NUMBER OF PAGES 54
		15. SECURITY CLASS. (of this report) Unclassified
		15a. DECLASSIFICATION/DOWNGRADING SCHEDULE
16. DISTRIBUTION STATEMENT (of this Report) Unlimited		
17. DISTRIBUTION STATEMENT (of the abstract entered in Block 20, if different from Report)		
18. SUPPLEMENTARY NOTES		
19. KEY WORDS (Continue on reverse side if necessary and identify by block number) Acoustic bottom interaction Digital data base Long range acoustics Topography		
20. ABSTRACT (Continue on reverse side if necessary and identify by block number) This report represents an assessment of sea floor and sub-sea floor relief as related to acoustic bottom interaction. Marine topography, whose amplitude spans six orders of magnitude, is here divided into three broad categories: (1) features likely to cause propagation blockage, (2) features which act as sloping bottoms, and (3) features which act as acoustic scatterers. Maps of the North Atlantic and North Pacific Oceans are presented which delimit the areas where each of these three categories would be expected to dominate propagation.		

DD FORM 1 JAN 73 1473

EDITION OF 1 NOV 68 IS OBSOLETE  
S/N 0102-LF-014-6601

Unclassified

SECURITY CLASSIFICATION OF THIS PAGE (When Data Entered)

392773

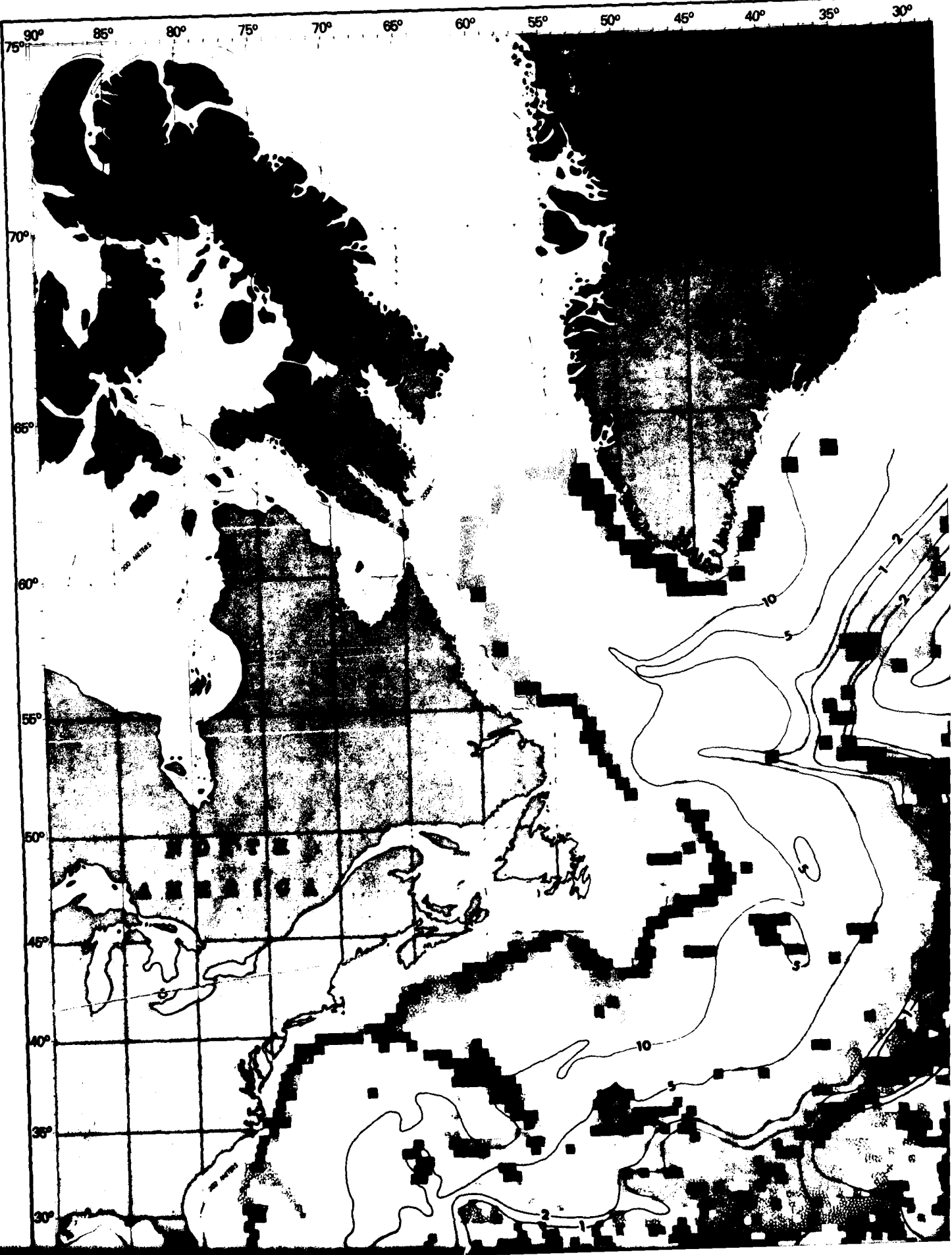
Unclassified

SECURITY CLASSIFICATION OF THIS PAGE (When Data Entered)

It is recommended that features causing blockage be dealt with in a deterministic manner based upon the best available bathymetry. Features producing a sloping bottom are often too small to be dealt with as individuals, and therefore have been dealt with statistically. It is demonstrated that this scale of relief can, at least as a first approximation, be treated as a stationary, stochastic process consisting of colored noise with a Gaussian distribution. A statistical model of features which act as scatterers was not developed. This class of relief, because of its size, requires stabilized, narrow-beam or deep-towed bathymetry for accurate definition. These features are the result of igneous, sedimentary and tectonic processes, and must, when collectively dealt with, have nonstationary statistics. For these two reasons, it is recommended that a more detailed assessment of acoustic requirements be made before major studies of this scale of relief are undertaken.

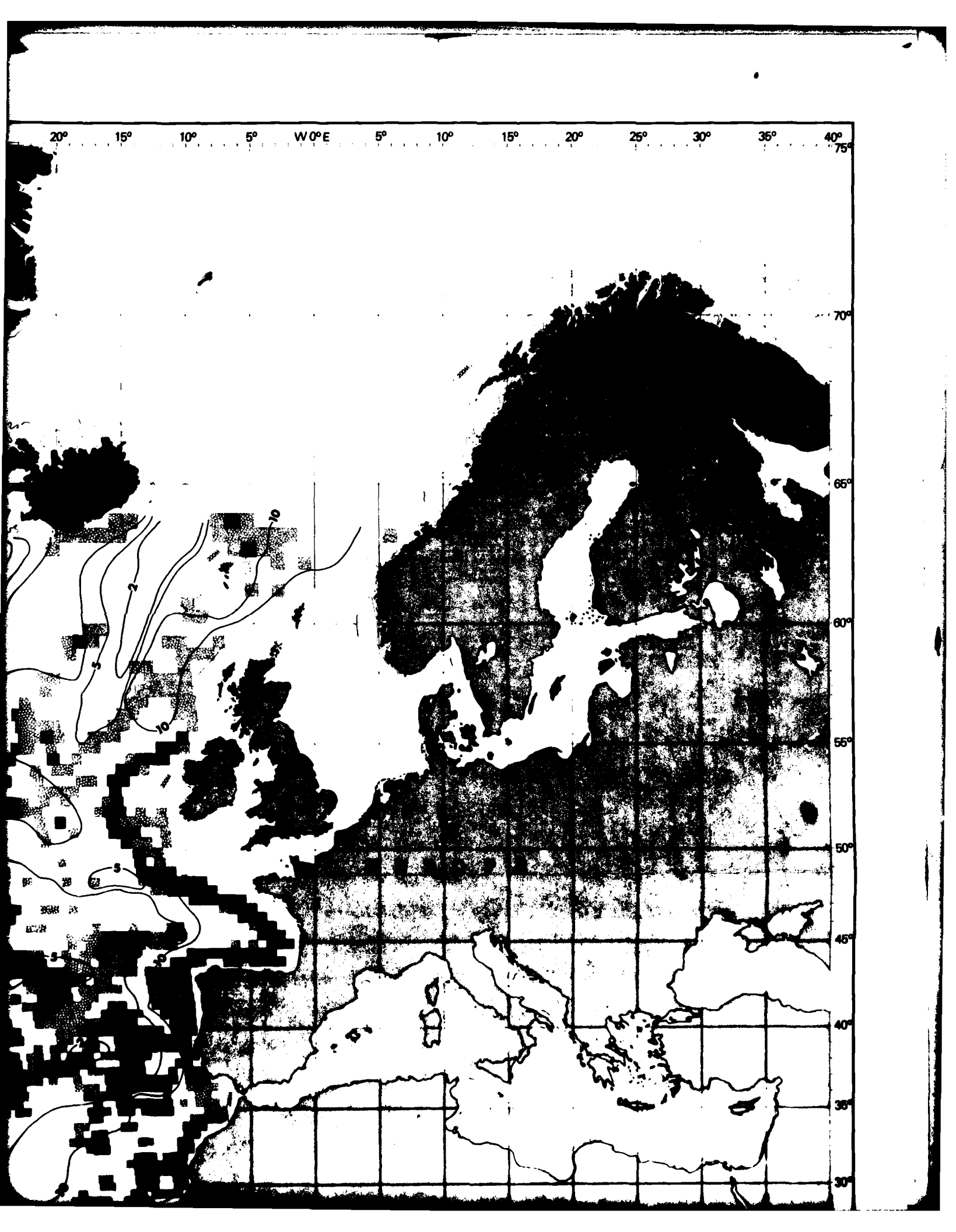
Unclassified

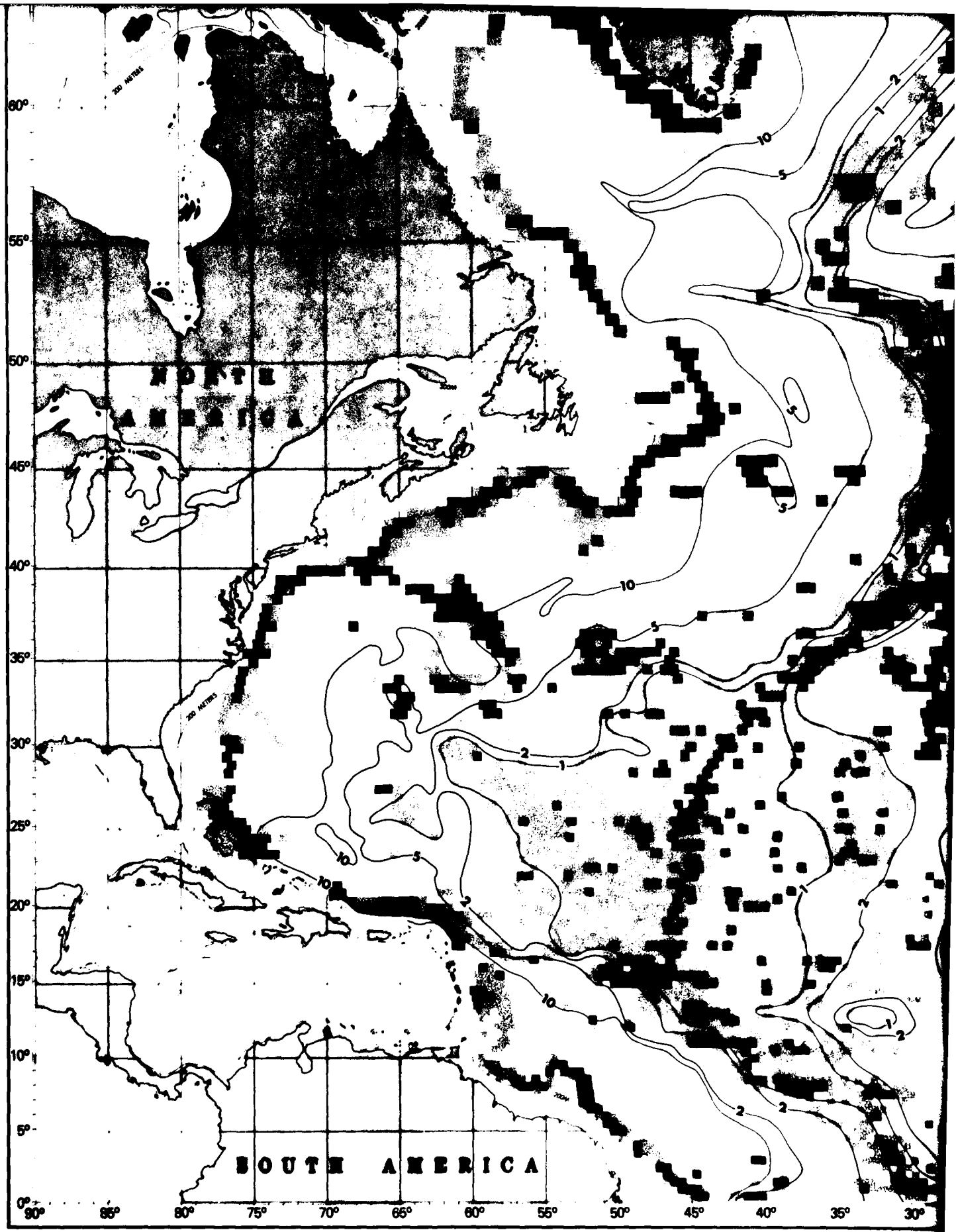
SECURITY CLASSIFICATION OF THIS PAGE (When Data Entered)



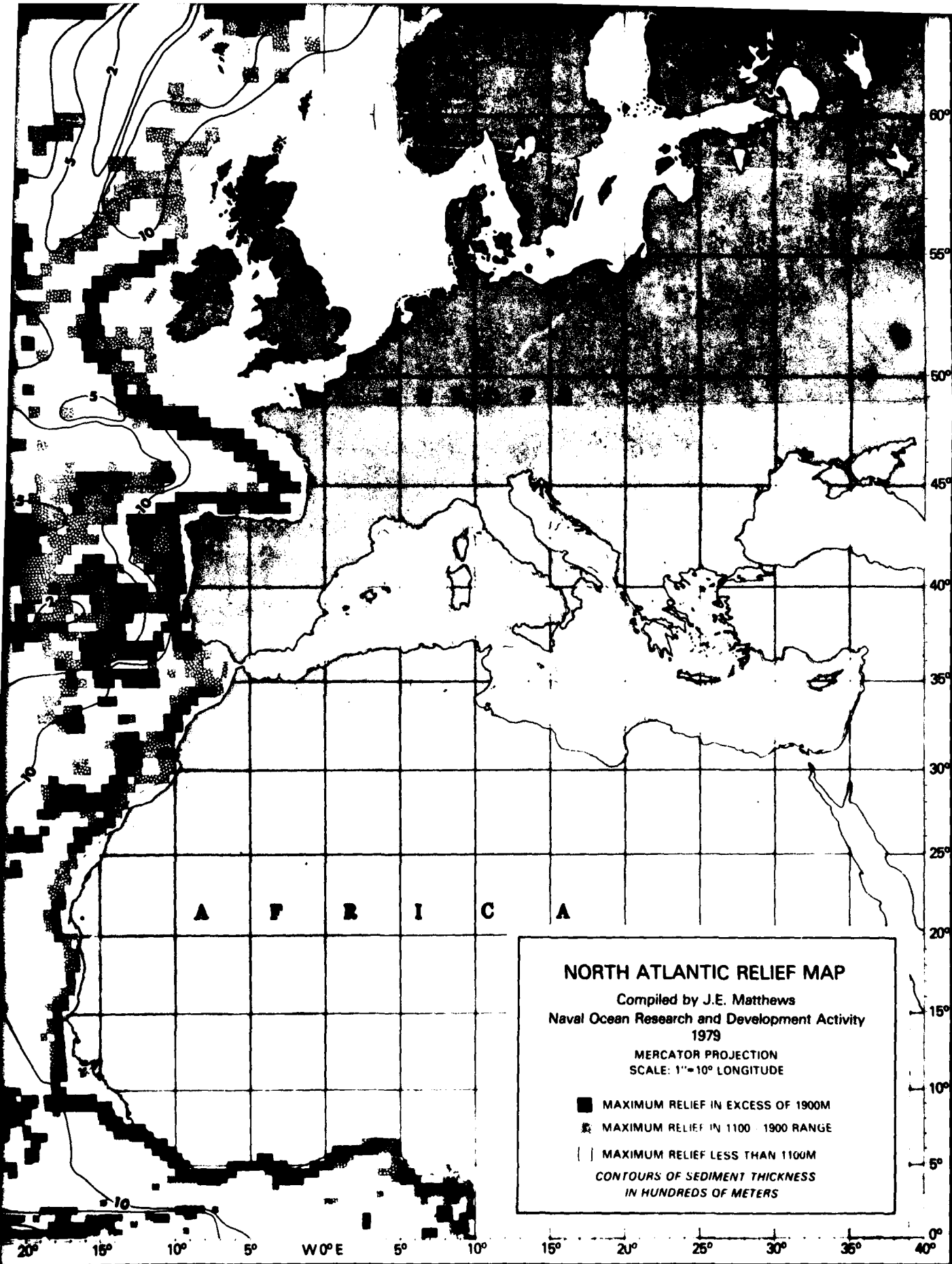
36° 30° 25° 20° 15° 10° 5° W 0° E 5° 10° 15° 20° 25° 30° 36°











### NORTH ATLANTIC RELIEF MAP

Compiled by J.E. Matthews  
Naval Ocean Research and Development Activity  
1979

MERCATOR PROJECTION  
SCALE: 1" = 10° LONGITUDE

- MAXIMUM RELIEF IN EXCESS OF 1900M
  - ▣ MAXIMUM RELIEF IN 1100 - 1900 RANGE
  - | | MAXIMUM RELIEF LESS THAN 1100M
- CONTOURS OF SEDIMENT THICKNESS  
IN HUNDREDS OF METERS

20° 15° 10° 5° W 0° E 5° 10° 15° 20° 25° 30° 35° 40°

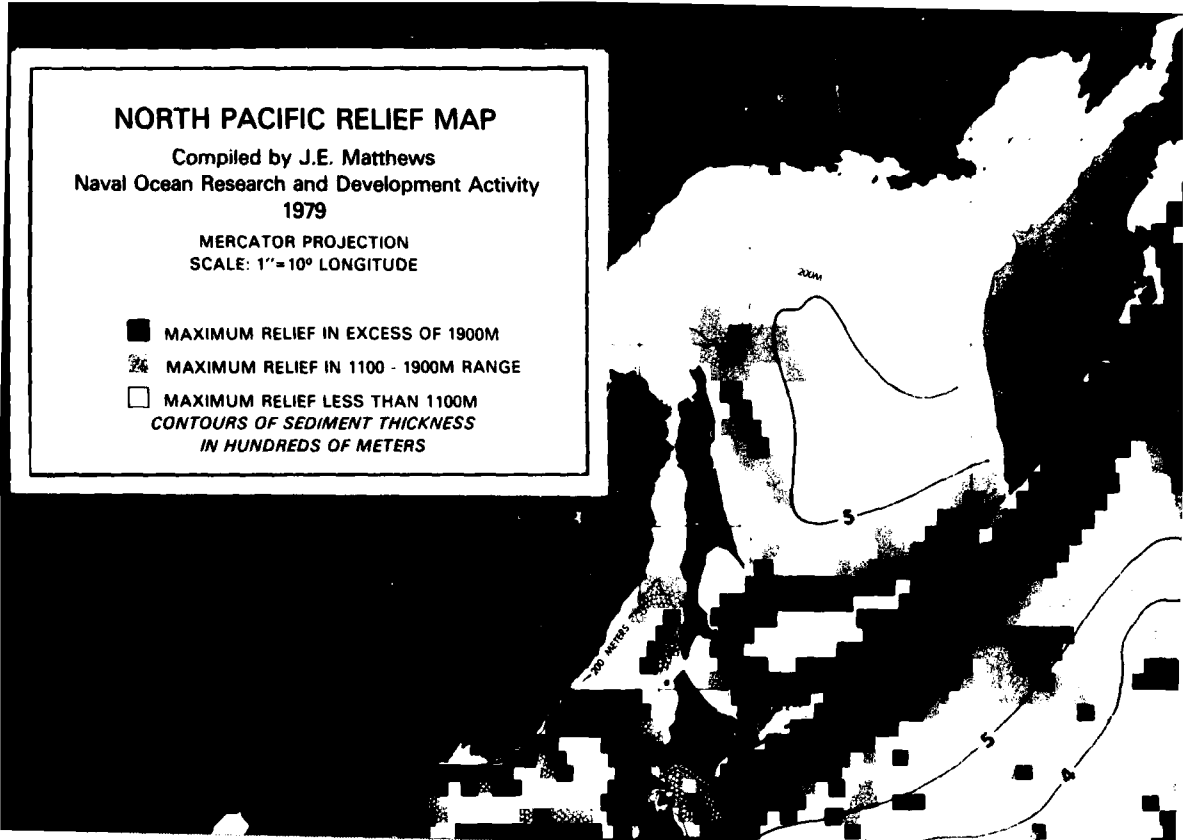
60°  
55°  
50°  
45°  
40°  
35°  
30°  
25°  
20°  
15°  
10°  
5°  
0°

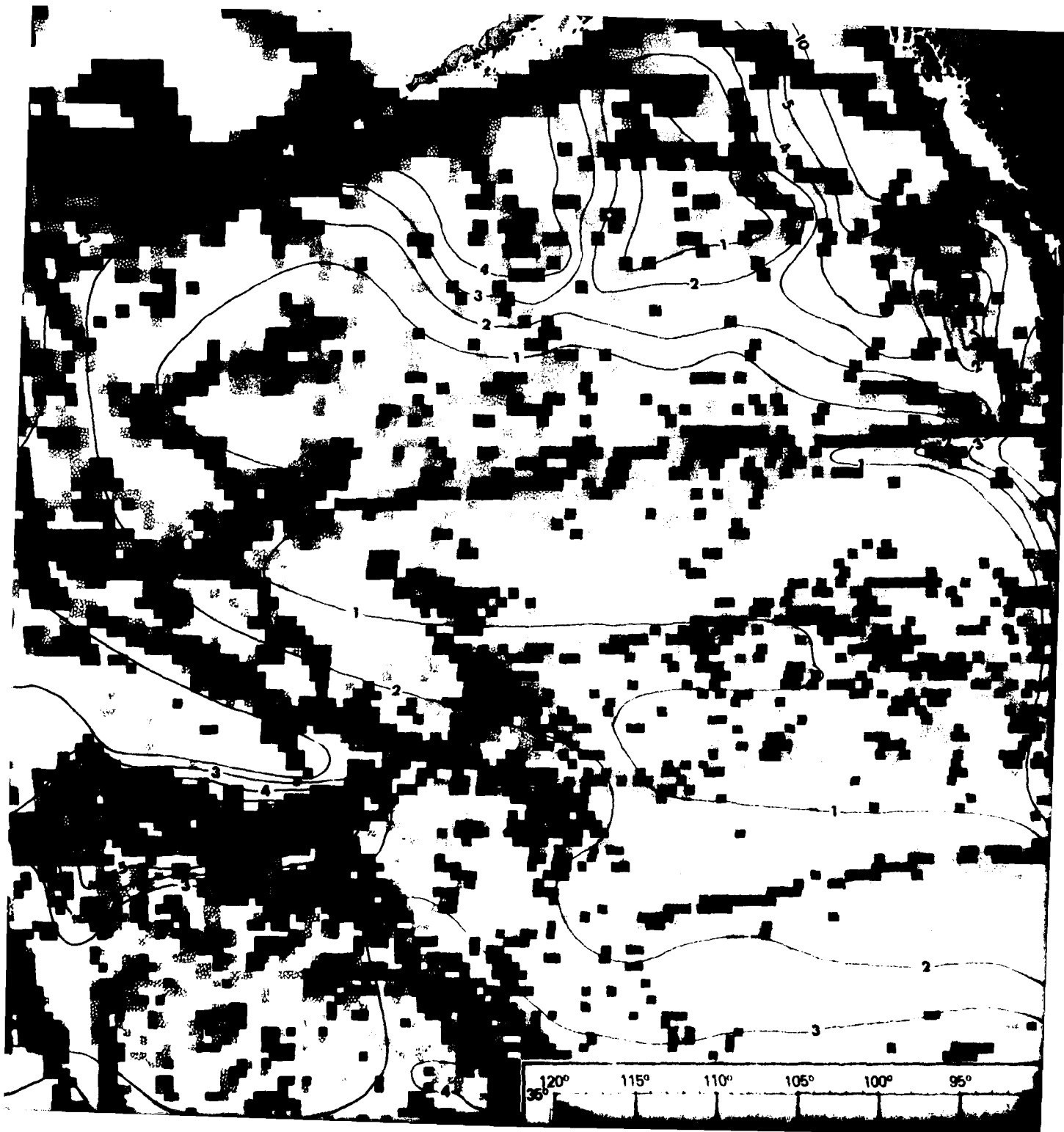
# NORTH PACIFIC RELIEF MAP

Compiled by J.E. Matthews  
Naval Ocean Research and Development Activity  
1979

MERCATOR PROJECTION  
SCALE: 1" = 10° LONGITUDE

- MAXIMUM RELIEF IN EXCESS OF 1900M
  - ▨ MAXIMUM RELIEF IN 1100 - 1900M RANGE
  - MAXIMUM RELIEF LESS THAN 1100M
- CONTOURS OF SEDIMENT THICKNESS  
IN HUNDREDS OF METERS*

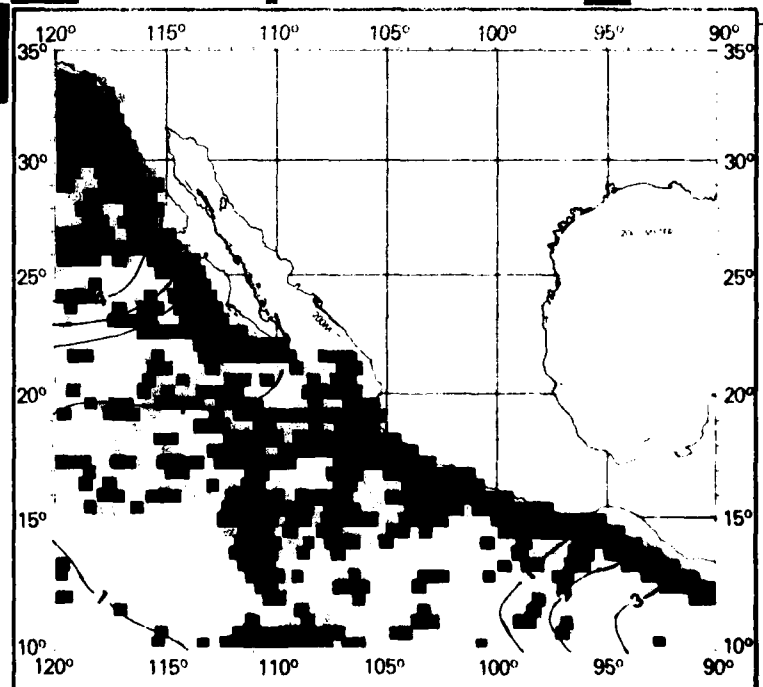
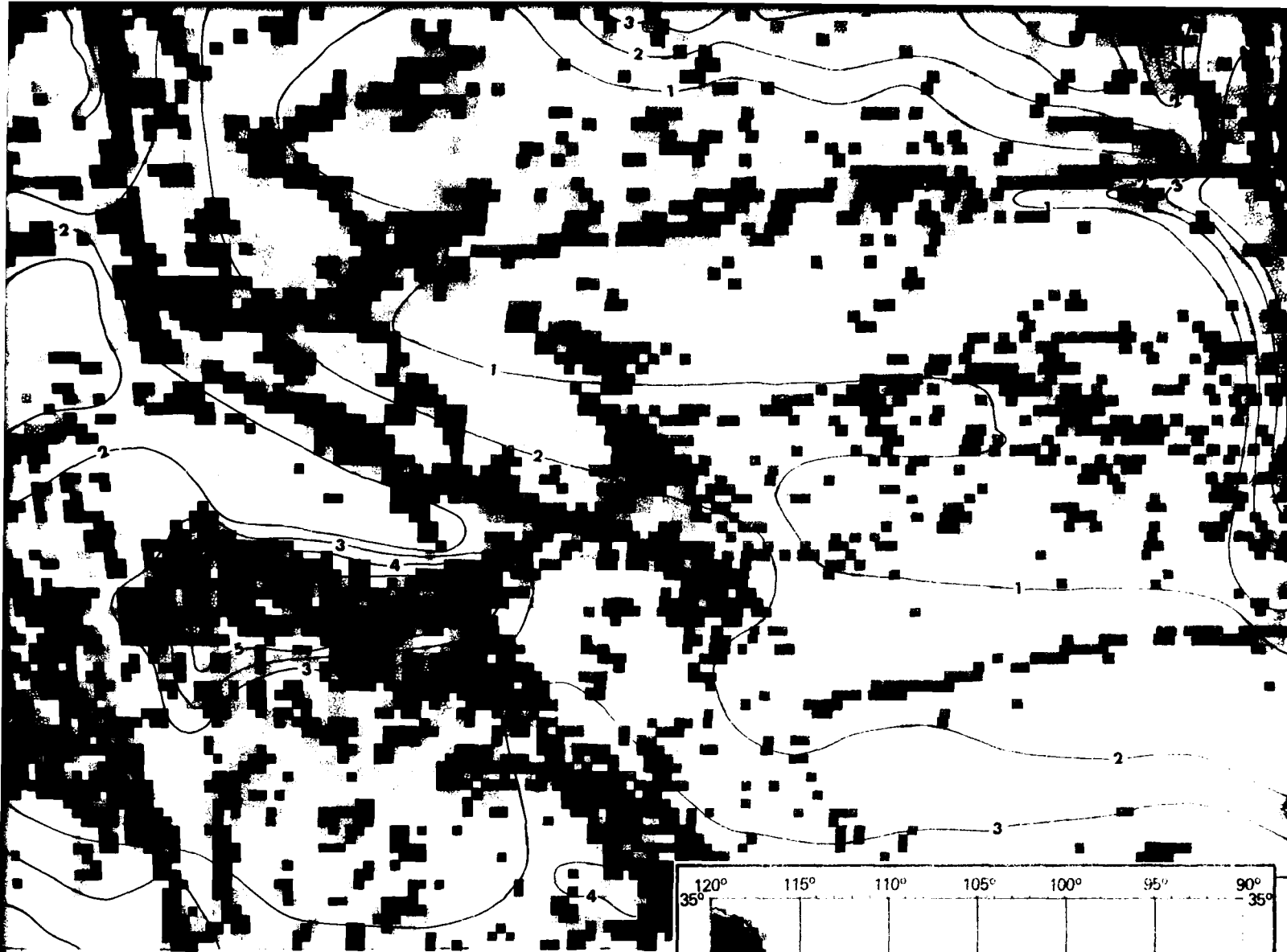




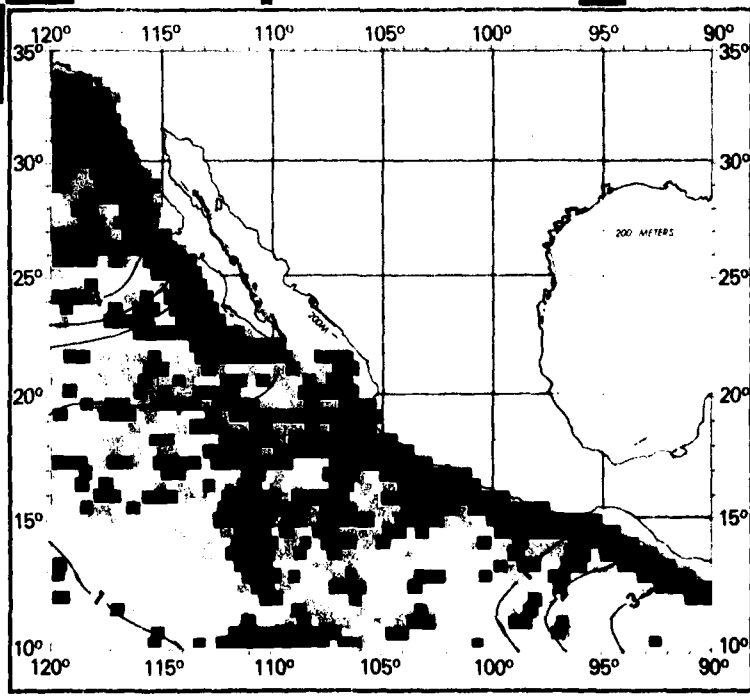
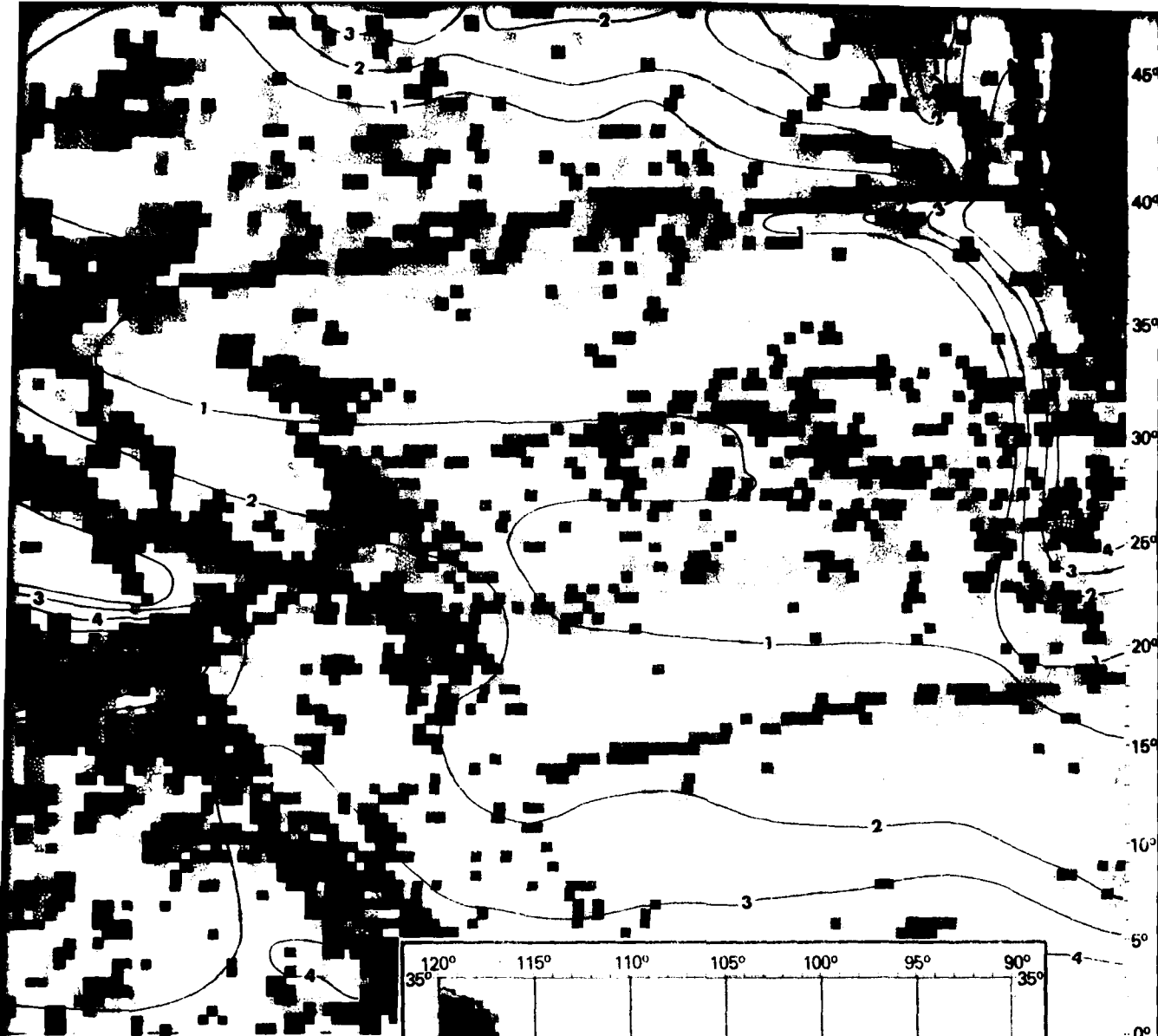




3



165° 170° 175° E 180° W 175° 170° 165° 160° 155° 150° 145° 140° 135° 130° 125°



175° 170° 165° 160° 155° 150° 145° 140° 135° 130° 125° 120°